Thesis (Spring 2016)

Report on

Optimal Energy Rendering Approach from Lightning Return Stroke

Submitted to the Department of Electrical and Electronic Engineering

Of

BRAC University

By

A.S.M.MISHKAT HUSSAIN CHOWDHURY 12121045

MD.SAKIB HOSSEN 12121156

HUMAIRA TABASSUM 12121148

Supervised by

Dr. A. K. M. Abdul Malek Azad

Professor

Department of Electrical and Electronic Engineering

BRAC University, Dhaka.

In partial fulfillment of the requirements for the degree of

Bachelor of Science in Electrical and Electronic Engineering

Spring 2016

BRAC University, Dhaka

Declaration

We hereby declare that the thesis titled "*Optimal Energy Rendering Approach from Lightning Return Stroke"* is submitted to the Department of Electrical and Electronic Engineering of BRAC University in partial fulfillment of the Bachelor of Science in Electrical and Electronic Engineering. This is our original work and was not submitted elsewhere for the award of any other degree or any other publication.

Signature of Supervisor

……

Dr. A. K. M. Abdul Malek Azad

Signature of Authors

……

A.S.M. Mishkat Hussain Chowdhury

……

MD. Sakib Hossen

……

Humaira Tabassum

Acknowledgements

We would like to take this opportunity to express our gratitude to all those who helped and supported us throughout this thesis project. We are cordially grateful and obliged to our supervisor Dr. A.K.M Abdul Malek Azad, Professor, BRAC University to allow and encourage us to work in this project. It would not be possible for us to complete this project without his constant encouragements, valuable insight, motivations, and guidelines. We would like to express our heartiest felicitations for his precious contribution.

Table of contents

List of figures

List of Tables

ABBREVIATIONS

CG- Cloud to Ground

IC -Intracloud

NLDN- (U.S. National Lightning Detection Network TM)

ARM- Advanced RISC Machine

GPS- Global Positioning System

PMT- Photomultiplier Tube

IIR- Infinite Impulse Response

IGBT- Insulated Gate Bipolar Transistor

MDF- Multidelay filtering

ToA- Time of arrival

Abstract

On emergent demand for a new source of efficient energy, a new source of renewable energy from lightning return stroke is a possible contributor to solve the energy crisis. The main objective of this study is to overcome the limitation and problems with detection, harvesting the lightning energy and store within a very short time. For detection purpose, based on the real time lightning detection system, light and infrasonic sound of lightning is used, and infrasonic sound is used for software designing to detect the lightning. With the help of Marx Generator a mock lightning is developed and a mathematical model is incorporated to understand and determine the characteristics of lightning through comprehensive simulation. Regarding the storage segment a high speed switching circuit is blueprinted and simulated with the help of Microcontroller and IGBT to store the energy in super capacitors within the desired time. The driving principal and software design of the proposed system are clarified in this paper. The simulation results corroborate the potency of the schemed method.

Chapter 1

Introduction

Since the commencement of human civilization energy has been a driving factor .But there is always a hunt for the energy sources as it is the base of all sort of development. Fossil fuel and the other natural resources has been the key which mitigated the all demand in last few decades. But, all the natural resources stash has an end. To mitigate the demand in the upcoming days a relentless research is going on about the renewable energy. But not all of the renewable energy sources are that much efficient & has some other problem as well. In this situation an alternative renewable energy like lightning return stroke may be the solution for new evolution. In addition rate of lightning occurs 100 flashes per second around the globe. Roughly 2000 thunderstorms are in progress over the earth's surface at any given time. The longest lightning observed was 120 Km long and stayed for 2 s [6]. One flash of lightning are equal to four strokes where each stroke has approximately one gigawatts that means around 1000 MW can be harnessed from just one stroke[5]. But there are lots of challenges for gaining the energy regarding the detection, storage etc. To come up with the challenges the mentioned approaches would be exhilarating.

1.1 Motivation:

Our country is burdened with over population with very few natural resources like gas, coal and few others. The energy crisis is hue and cry for us and a impediment for our development as well. If there is no invention of new resources found in our country we are going to dry of resources within few decades. In fact we even started to purchase electricity from our neighboring countries which intensifies the crisis. Use of renewable energy is very low in our country. With respect to the total it is just only 3.23% of the total generation [6]. The expectancy from the coal is not so high and among the renewable energy Nuclear is approximated to be future base load option but it consist very high risk and cost and the maintenance is quite dreadful. Except these the waste management of nuclear plant is still not planned. For these sort of crisis problem, quick rental power plant is growing very fast which in fact destroying our economy. Lack of electricity creating hazard like load shedding, production problem, attenuation in agriculture hampering the studies and what not. To, mitigate these blazing issues only a new source of renewable energy from lightning return stroke can contribute up to the mark.

Chapter 2

Lightning Detection

In recent years lightning detection technique has got innumerable progress throughout the world. Several methods and different techniques are used widely to get a better result in case of lightning. For the purpose of generating electricity from the lightning return stroke, detection of lightning is quite indispensable. For this purpose at first we have done a comparative analysis amongst the lightning detection systems and networks which has been developed recently. The detection systems are based on CG (Cloud to ground) lightning as our concern is only on CG lightning. Then we have done a simulation regarding the detection of lightning based on infrasonic sound with the help of Lab VIEW software.

2.1 Lightning Theory

Transient and high current discharges are measured in kilometers in lightning path length. Intracloud discharges and cloud to ground discharges are occurred much more than cloud to cloud and cloud to air. As cloud to ground lightning is concern for us in all-purpose so this specific form is viciously studied. In the distribution of charges in the cloud, negative charges are collected at the bottom and positive at the top. Charges at the bottom of the cloud draws and equal in magnitude but opposite polarity charge at the ground level which turns into capacitor system between cloud and the ground where the dielectric is air [5]

The majority of CG flashes embark from the intracloud (IC) and after a few part of second this come down as a negative charge along the channel, very few carries the negative. An intense

positive wave of ionization actually defines the return stroke which discharges upward through the channel at about the half speed of light. There are several strokes in a CG flash and it hangs about half of a second [1].

2.2 Comparative Analysis among The Lightning Detection Method

2.2.1 NLDN Method

At first we are going to describe briefly about the NLDN method (U.S. National Lightning Detection Network TM). Individual return stroke of CG flash radiation are sensed by this system. Around four million square miles and peaks, up to 14000 feet (4300 m) are considered in this method which also includes electrical conductivity ranges from 1 to above 30 ms/m, where 0.1 flashes/km^2 to 20 flashes/$km^2$are the flash densities. The NLDN consist of 47 IMPACT sensors and 59 upgraded LPATS-III sensors where these sensors been upgraded several times to allow the detection area beyond 500m and to avoid nearby cloud discharges. The data acquisition take 30-40 s of each lightning flash in this method via a two way satellite communication system, but in satellite broadcast link we only get the CG flash data with 0.1-s time resolution. Several error like “DF site errors” or systematic errors in magnetic direction could take place in real time NLDN data which could subsequently eliminated by applying appropriate modification. This method uses MDF and ToA algorithm which actually uses a least-squares optimization procedure to compute flash locations in real time [1].

Peak signal amplitudes are used in NLDN to measure the peak current. Flash detection accuracy determines the ability of a network for detection of CG lighting. It shows various range of efficiency for different peak value. For greater than 16KA DE of about 97% (38 out of 39); for 6-10 kA range it is 15% and 0 for lower than 6kA.The median accuracy of NDLN is found to be 500 meter. From the above discussion we can come up to the summary that NLDN can detect each return stroke of a CG flush if it exceeds the nominal peak current with quite good efficiency [1].

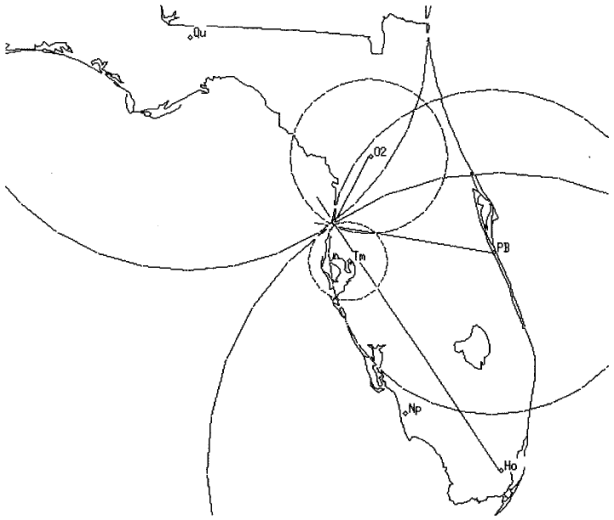

Figure 2.1: Example of a return stroke that was located by two LPATS sensors(circle only) and three IMPACT sensors (circles and vectors). (Adapted from [1].)

2.2.2Lightning detection system based on ARM

Secondly, we are going to describe briefly about Lightning Detection System Based on ARM. For this system a novel Rogowski Coil is designed to use signals by collection module to detect the lightning. A master controller STM32F103ARM is incorporated if there are option for SD card module, time module and display module. In overall system it includes 32 bit microcontroller which is the key thing, lightning signal acquisition module, display and control module, SD card storage module and the PC which works as a host machine. In the time of lightning, signal acquisition module awaken the microcontroller with a respective pulse [2]. For this method master chip has a certain configuration which is "Cortex-M3 core, high-performance, low-power, real-time characteristics, the operating frequency of72MHz, the built-in high-speed memory, 12-bit AD converter, SDIO driver module, timer connected to the outside via the APB bus set , 80 I / O interfaces and up to 128KB flash memory and 20KB SRAM, and it provides three kinds of low power modes for the user to optimize power consumption reasonably" [use the no 5 ref of arm paper] . Shunts and Rogowski coil are the two ways through which lightning signal acquisition can be done. Here this coil able to measure 3-150kA, and

wave current changes from 1/10 us to 20/500 us. The output of the lightning current between 0-3.5 A, and sampling voltage between 0-3.5 V and output sensitivity can make about 0.57V/kA, which convene the most lightning measurement necessities. Rogowski coil uses a special protection against excessive current resistance through using bridge rectifier and filter circuit, where the filter is LC-II type and capacitor composed of inductor core. Here, Microcontroller software can compensate and correct about 90% of the initial value. In order to protect the data acquisition module from the lightning environment opt coupler components HCNR201 is used which has high linearity, wide bandwidth; low-temperature coupler can perform a variety of photoelectric conversion circuit isolation. RS485 another bus communication integrated with fast switching is used to protect against lightning overvoltage. From the system test and analysis it was found that coefficient of variation for different impact current coil is basically stable at 1635A/V vicinity within a allowable error range of fine linear relationship. The maximum measurement error is 0.37% for this system. Certain range of intensity can be identified by this system which in total illustrates that not only counting the time of lightning but also this system is even capable to monitor the intensity of lightning and the lightning current waveforms [2].

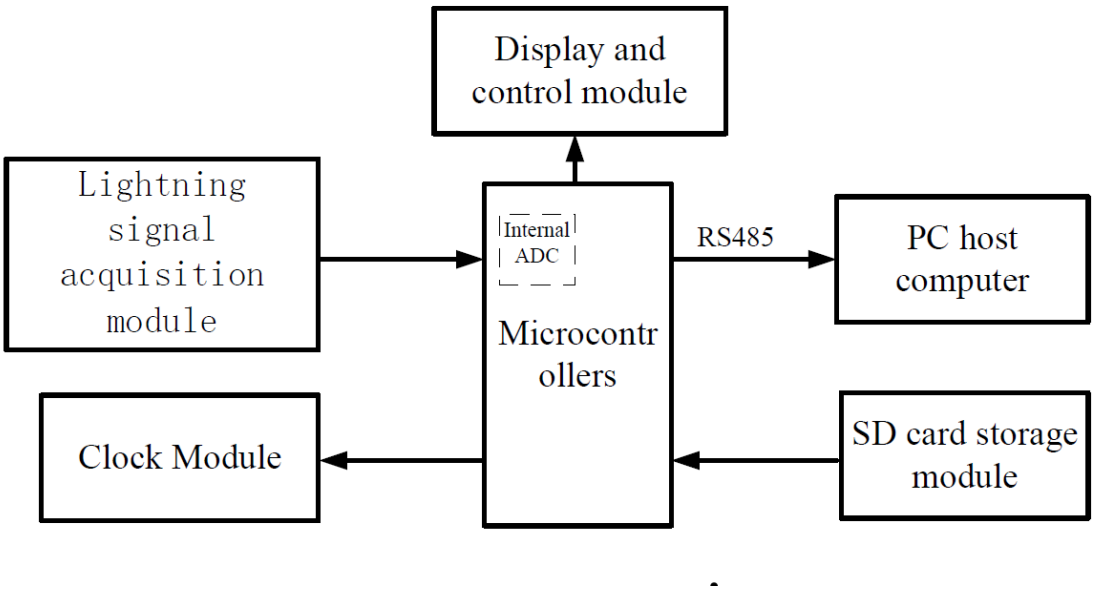

Figure 2.2: Overall ARM system framework

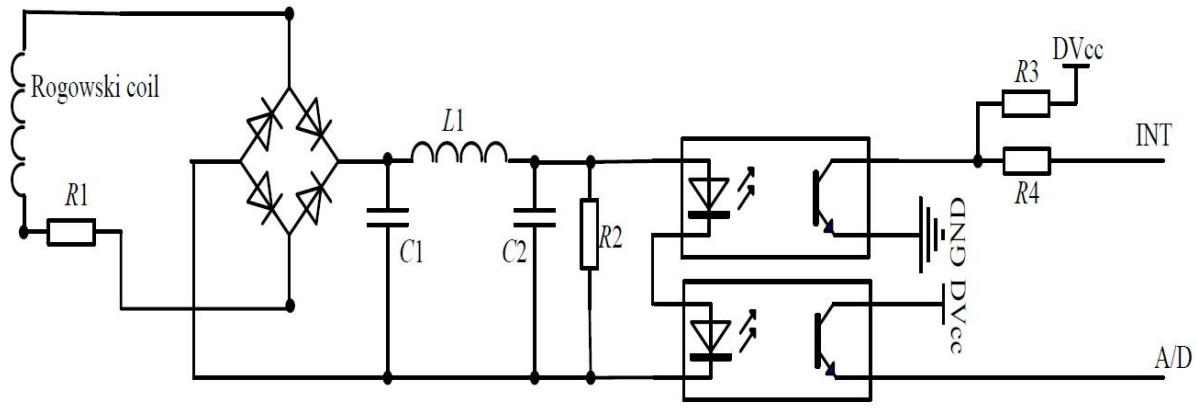

Figure2.3: Lightning signal acquisition module circuit diagram

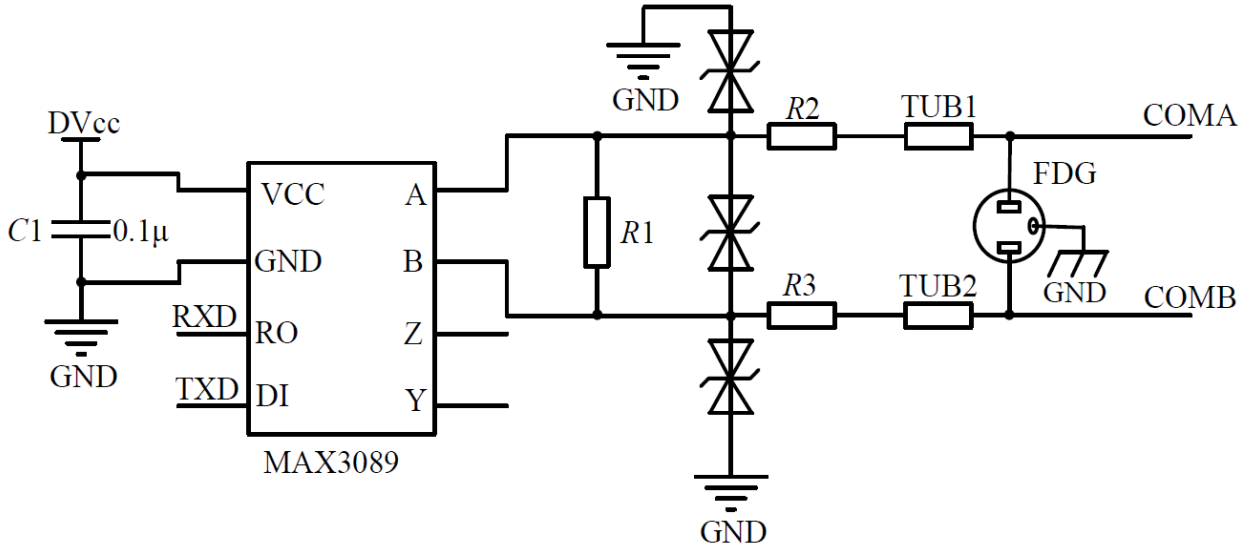

Figure 2.4: RS-485 bus communication has lightning protection technology circuit diagram

2.2.3 Lightning Detection system based on Photon and Infrasonic Sound

Finally, we are going to illustrate the detection method based on Photon and Infrasonic sound. Among the three systems actually we preferred this system and simulated part of it using Lab VIEW software. Because this system is less complex and more efficient for our purpose of storing the energy of lightning. In previous days lightning location system were expensive because it was based on electromagnetic radiation, but this system reduce the cost as well. The

design is based on two factors; visible light and ultraviolet light, which irradiation from the highly ionized lightning channel and thunder from a sudden and intense heating of the air in the lightning channel that are decoded by number of Photomultiplier tubes and acoustic sensors. Remote display and control can be done through a host computer and LabVIEW software. This system is multifunctional which can be divided into separate blocks for individual purpose. It consists with Photon detection system, Infrasound detection system, Data acquisition system and GPS remote display system.

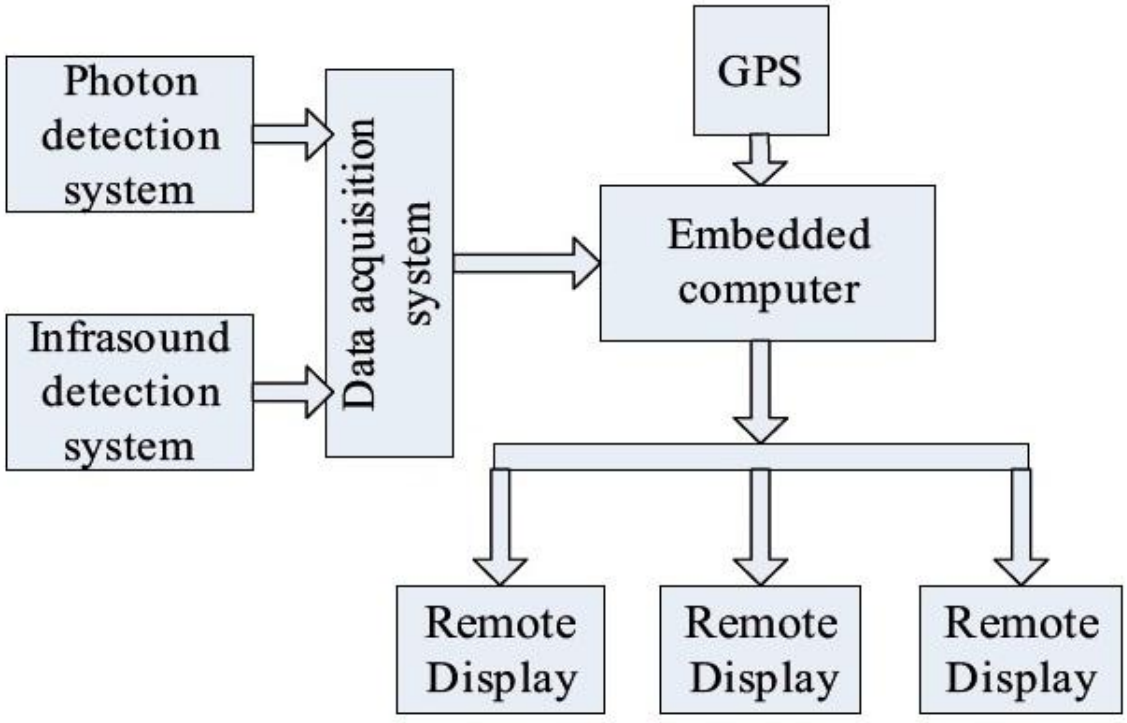

Figure2.5: Block Diagram of Lightning Locating system

Inside the photon detection units there are eight photomultiplier tubes (PMT), voltage biasing circuit and signal modulate circuit. Outside photoemission is the basis for this vacuum photo electric sensor named as PMT. For detecting the faintness and fast response of light signal PMT can be used as it is highly sensitive and have rapid response speed. In the eight directions eight PMTs are oriented. A lightning signal is obtained by eight PMTs, and then it is converted into voltage signal with limited amplitude by outside circuit. DAQ card coupled with the system deliver this data to the embedded computer where the computer compute the correct azimuth due to the variation of orientation's voltage input [3].

Figure2.6: Photomultiplier tube GDB-221 developed by Yufo Electronics

Figure 2.7: C9692 Photon detection unit developed by HAMAMATSU

Infrasound detection unit consists of infrasound sensors, transform circuit and signal pretreatment circuit. As we got to know that Infrasound is the main proportion of the whole thunder and its main frequency range is between 1.3 Hz to 6Hz. and the most dominant frequency is 3.5 Hz. Wind, Typhoon, earthquake, volcano eruption and many other natural sources creates infrasound. So, multilevel of filtering is needed to distinguish the signal of lightning. NI DAQ card with 16 bits input resolution and 250K max sampling rate is needed for this purpose. With the accuracy about 1 μs GPS clock provides the synchronization of the signals and it is responsible for both lightning signal synchronization and time of arrival lightning location with the help of multi station system. After a lightning comes, PMT first acquire the light signal and after a while infrasound sensors receive it. Eight channels light signals are calculated to lightning flash azimuth and GPS clock is combined to calculate the time between light and infrasound arriving, from where we could calculate the flash distance. For computing exact longitude and latitude to orientation this data can be used. For the Data acquisition purpose

NI Lab VIEW offers three stages of driver software, among those, NI-DAQmx is used for its full feature high performance. After data acquisition and signal treatment from the PMT precise azimuth are computed through Math Script node. Synthesizing the both azimuth and distance the specific position of longitude and latitude of lightning are detected. For remote communication and display LabVIEW provides unique and distinguished features which also allow to remote display of the collected data [3].

2.3 Signal Analysis and Software design of the system using Lab VIEW based on Infrasonic Sound

LabVIEW is a graphical programming language that uses icons instead of lines of text to create applications. Actually the dataflow programming is used by LabVIEW. In LabVIEW a user interface is built with set of tools and object which is known as front panel. Then the front panel can be manipulated by coding. The block diagrams are belonging to this code and some ways it represents the flowchart as well.

As the lightning has wide band of frequency so it is interfered by almost all sorts of signals. Forms of noise are widely varied from local, non-acoustic pressure, atmospheric boundary layer,

natural sound sources and etc. Except the others tornado, wind, earthquake and few other source has very close range of frequency near to the lightning frequency. A special types of filtering is needed to gather the bandwidth of lightning. Firstly the signal is sampled 1000 times, means 1000ms within 1 sample gives us a cycle. For adding the noise sync function is introduced which has got input from the multiplication with sample frequency and loop iterator. A noise is generated by Rand function which is multiplied with a constant and later it is added with the Sinc function. So this thing gave us the curve with noise. At first we sorted a graph without noise named as sampling graph. As we need to detect the infrasonic sound so we used a special type of IIR(infinite Impulse Response) filter named butterworth filter. IIR filter are also known as recursive filter. The IIR filter not only uses input values but also uses previous output values. The following general difference equation characterizes IIR filters

$$y_i = \frac{1}{a_0}\left(\sum_{j=0}^{N_b-1} b_j\, x_{i-j} - \sum_{k=1}^{N_a-1} a_k\, y_{i-k}\right)$$

Where $b_j$is the set of forward coefficients is, $N_b$is the number of forward coefficients, $a_k$is the set of reverse coefficients and N_a is the number of reverse coefficients, where X_i is the current input, X_{i-j} is the past inputs and Y_i-k is the past outputs [4].

The below equation defines the direct form transfer function of an IIR filter

$$H(z) = \frac{b_0 + b_1 z^{-1} + \cdots \ldots \ldots b_{N_b-1} z^{-(N_b-1)}}{1 + a_1 z^{-1} + \cdots \ldots + a_{N_a-1} z^{-(N_a-1)}}$$

Where a_n and $b_n$are the reverse and forward coefficients of the IIR filter.

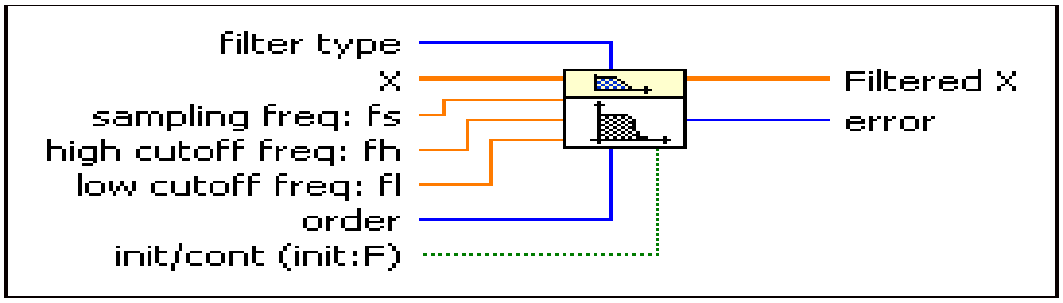

Figure2.8: Butterworth filter with all the input and output function

Reasons for using butterworth filter are several

- It provides the advantages of providing the higher selectivity for a particular order. Smooth response at all frequencies
- Monotonic decrease from the specified cut-off frequencies
- Maximal flatness, with the idea response of unity in the pass band and zero in the stopband.
- Half power frequency or 3 dB down frequency that corresponds to the specified cut off frequencies.

The transfer function of butterworth filter is given by-

$$B(w) = \frac{1}{\left[1 + \left(\frac{w}{w_0}\right)^{2n}\right]^{\frac{1}{2}}}$$

Where n is the order of the filter [4].

In the below simulation we used to consecutive filter. Firstly we used Butterworth filter as a low pass filter and secondly as a bandpass filter. Firslty it draws the frequency within 20 Hz and then we get our desired graph within the range from 1.3Hz as low cut-off and 6Hz as higher cut-off frequency.

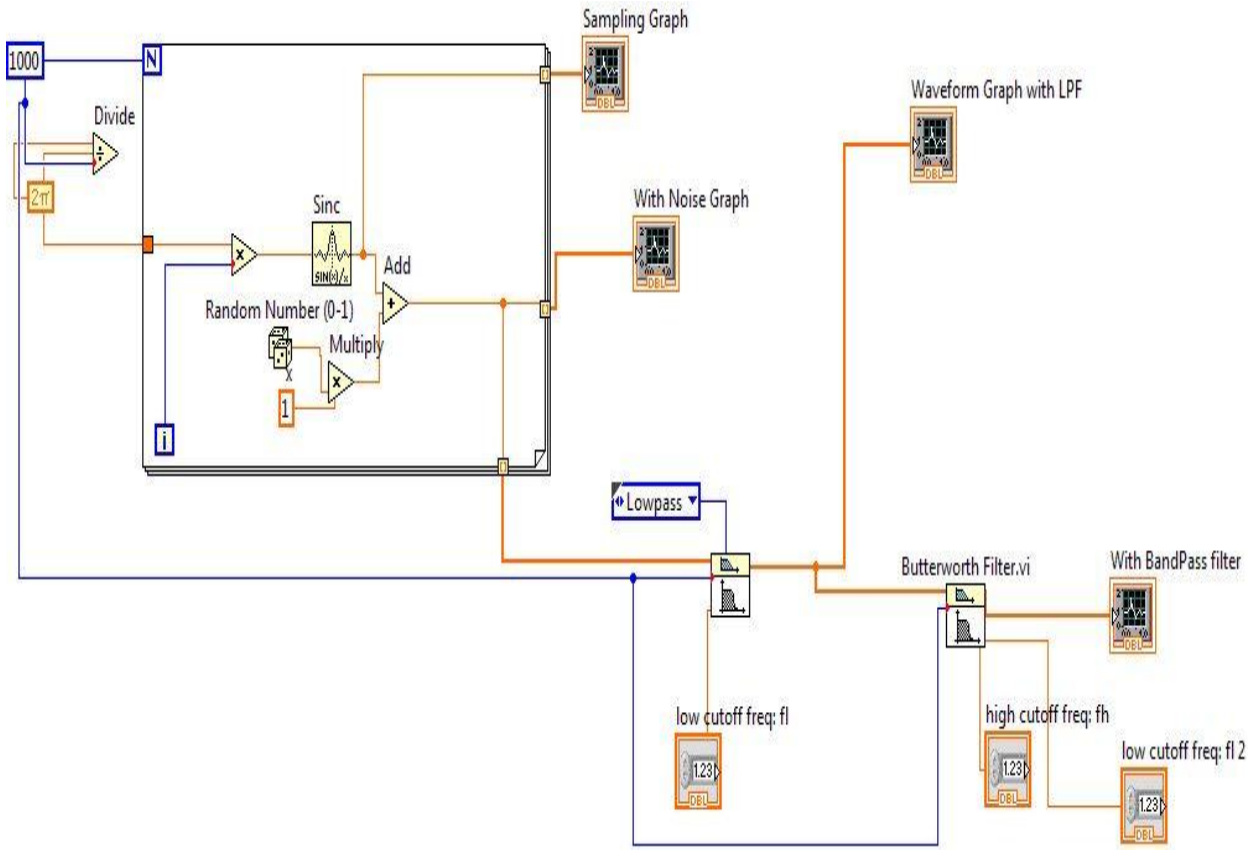

Figure2.9: Block diagram of infrasonic sound detection

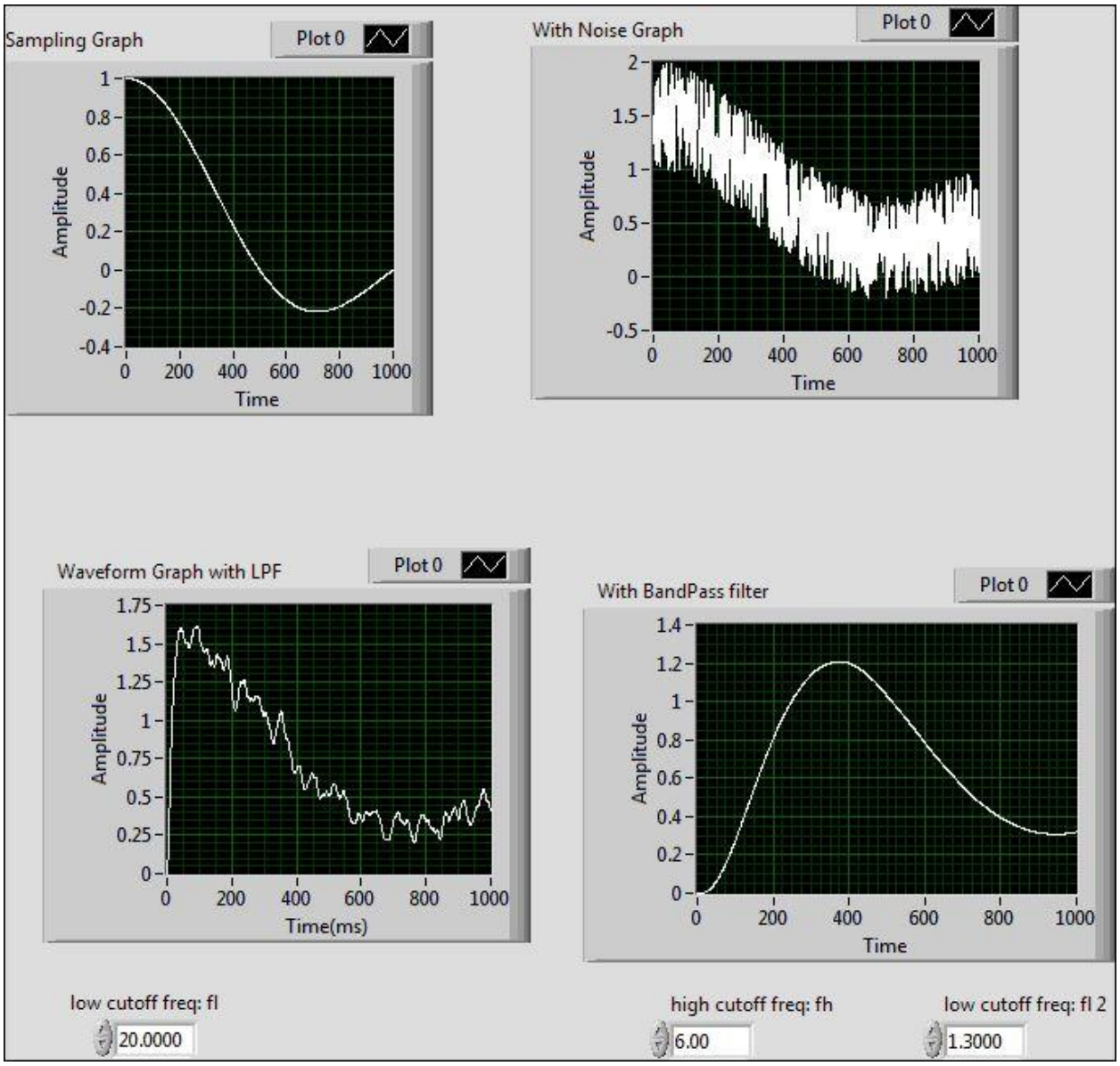

Figure 2.10: Respective curve got from the simulation

CHAPTER 3

Mathematical Model and Simulation of Marx Generator

3.1 High Voltage Impulse:

Disturbances of electric power transmission and distribution systems are frequently caused by two kinds of transient voltages whose amplitudes may greatly exceed the peak values of the normal a.c. operating voltage. The first kind are lightning over voltages, originated by lightning strokes hitting the phase wires of overhead lines or the bus bars of outdoor substations. The amplitudes are very high, usually in the order of 1000 kV or more, as every stroke may inject lightning currents up to about 100 kA and even more into the transmission line [7], each stroke is then followed by travelling waves, whose amplitude is often limited by the maximum insulation strength of the overhead line. The rate of voltage rise of such a travelling wave is at its origin directly proportional to the steepness of the lightning current.

Too high voltage levels are immediately chopped by the breakdown of the insulation and therefore travelling waves with steep wave fronts and even steeper wave tails may stress the insulation of power transformers or other h.v. equipment severely. Lightning protection systems, surge arresters and the different kinds of losses will damp and distort the travelling waves, and therefore lightning over voltages with very different wave shapes are present within the transmission system. The second kind is caused by switching phenomena. Their amplitudes are always related to the operating voltage and the shape is influenced by the impedances of the system as well as by the switching conditions. The rate of voltage rise is usually slower, but it is well known that the wave shape can also be very dangerous to different insulation systems, especially to atmospheric air insulation in transmission systems with voltage levels higher than 245 kV [8]. Both types of over voltages are also effective in the l.v. distribution systems, where

they are either produced by the usual, sometimes current-limiting, switches or where they have been transmitted from the h.v. distribution systems.

3.1.1 Standard Lightning Impulse Wave Shapes:

The actual shape of both kinds of over voltages varies strongly, it became necessary to simulate these transient voltages by relatively simple means for testing purposes. The various national and international standards define the impulse voltages as a unidirectional voltage which rises more or less rapidly to a peak value and then decays relatively slowly to zero. In the relevant IEC Standard 60[9]widely accepted today through national committees [10],a distinction is made between lightning and switching impulses, i.e. according to the origin of the transients. Impulse voltages with front durations varying from less than one up to a few tens of microseconds are, in general, considered as lightning impulses.

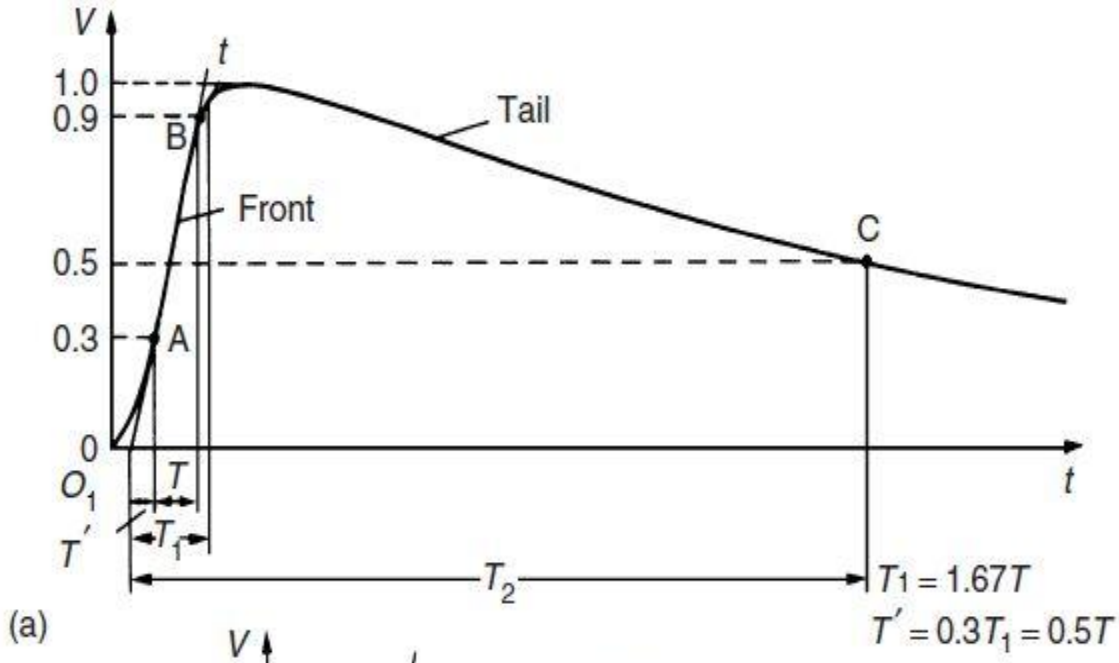
V
t
1.0
0.9
B
Tail
Front
C
0.5
0.3
A
0
O_1
T
T_1
T′
t
T_2
$T_1 = 1.67T$
$T' = 0.3T_1 = 0.5T$

(a)

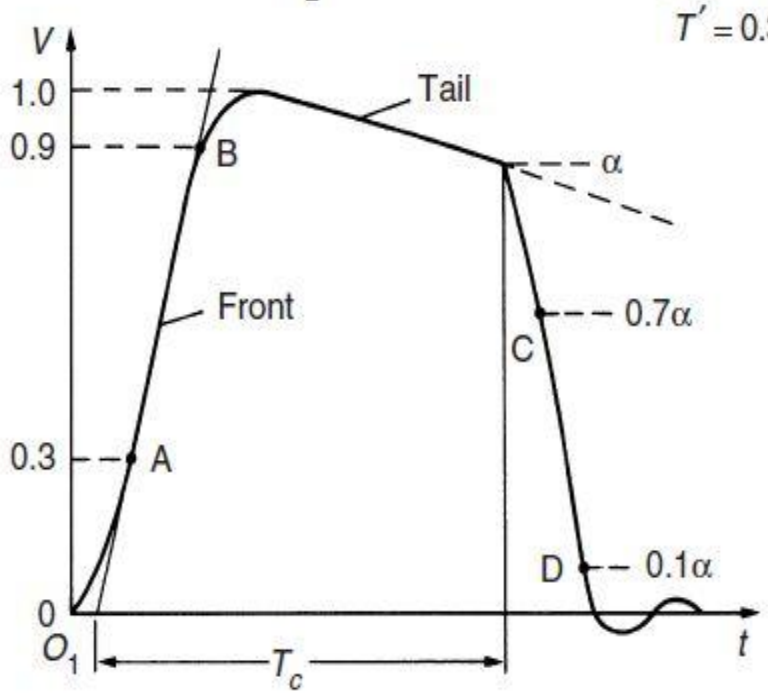
V
1.0
0.9
Tail
B
α
Front
0.7α
C
0.3
A
D
0.1α
0
O_1
T_c
t

(b)

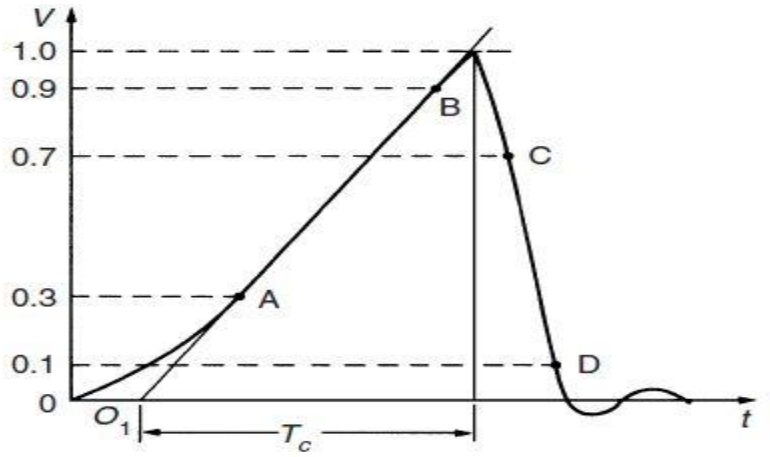

(c)

Figure 3.1 ***General shape and definitions of lightning impulse (LI) Voltages. (a) Full LI. (b) LI chopped on the tail. (c) LI chopped on the front.*** **T1*: front time.*** **T2*: time to half-value.*** **Tc*: time to chopping.*** **O1*: virtual origin***

Figure 3.1(a) shows the shape for such a 'full' lightning impulse voltage as well as sketches for the same voltage chopped at the tail (Fig. 3.1(b)) or on the front (Fig. 3.1(c)), i.e. interrupted by a disruptive discharge. Although the definitions are clearly indicated, it should be emphasized that the 'virtual origin' O1 is defined where the line AB cuts the time axis. The 'front time' T1, again a virtual parameter, is defined as 1.67 times the interval T between the instants when the impulse is 30 per cent and 90 per cent of the peak value for full or chopped lightning impulses. For front-chopped impulses the 'time to chopping' Tc is about equal toT1. The reason for defining the point A at 30 per cent voltage level can be

found in most records of measured impulse voltages. It is quite difficult to obtain a smooth slope within the first voltage rise, as the measuring systems as well as stray capacitances and inductances may cause oscillations. For most applications, the (virtual) front time T1 is 1.2 μs, and the (virtual) time to half-value T2 is 50 μs. In general the specifications [3]permit a tolerance of up to ±30 per cent for T1 and ±20 per cent for T2. Such impulse voltages are referred to as a T1/T2 impulse, and therefore the 1.2/50 impulse is the accepted standard lightning impulse voltage today. Lightning impulses are therefore of very short duration, mainly if they are

chopped on front. Due to inherent measurement errors and uncertain tiesin the evaluation the 'time parameters' T1, T2 and T_c or especially the time difference between the points C and D (Figs 3.1(b) and (c)) can hardly be quantified with high accuracy.

3. 2 Circuits for Producing Impulse Waves:

The introduction to the full impulse voltages as defined in the previous section leads to simple circuits for the generation of the necessary wave shapes. The rapid increase and slow decay can obviously be generated by discharging circuits with two energy storages, as the wave shape may well be composed by the superposition of two exponential functions. Again the load of the generators will be primarily capacitive, as insulation systems are tested. This load will therefore contribute to the stored energy. A second source of energy could be provided by an inductance or additional capacitor. For lightning impulses mainly, a fast discharge of pure inductor is usually impossible, as h.v. chokes with high energy content can never be built without appreciable stray capacitances. Thus a suitable fast discharge circuit will always consist essentially of two capacitors.In order that equipment designed to be used on high voltage lines, and others, be able to withstand surges caused in them during operation, it is necessary to test these equipment with voltages of the form likely to be met in service.

The apparatus which produces the required voltages is the impulse generator. In high voltage engineering, an impulse voltage is normally a unidirectional voltage which rises quickly without appreciable oscillations, to a peak value and then falls less rapidly to zero. A full impulse wave is one which develops its complete wave shape without flashover or puncture, whereas a chopped wave is one in which flash-over occurs causing the voltage to fall extremely rapidly. The rapid fall may have a very severe effect on power system equipment.

The lightning waveform is a unidirectional impulse of nearly double exponential in shape. That is, it can be represented by the difference of two equal magnitude exponentially decaying waveforms. In generating such waveforms experimentally, small oscillations are tolerated. Figure 2.2 shows the graphical construction of the double exponential waveform

$$v(t) = V (e^{-\alpha t} - e^{-\beta t})$$

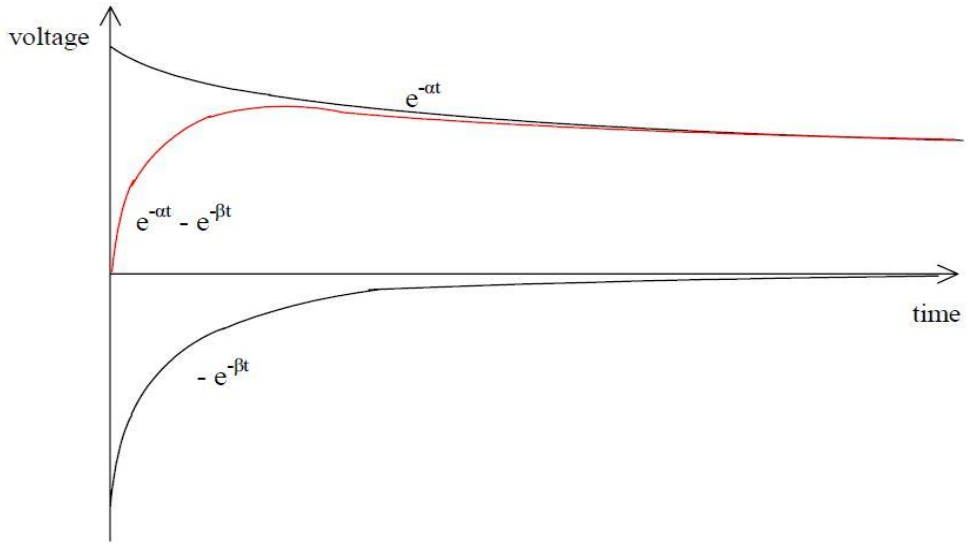

Figure 3.2 - Double exponential waveform

In most impulse generators, certain capacitors are charged in parallel through high series resistances, and then discharged through a combination of resistors and capacitors, giving rise to the required surge waveform across the test device.

3.2.1 Single-stage generator circuits:

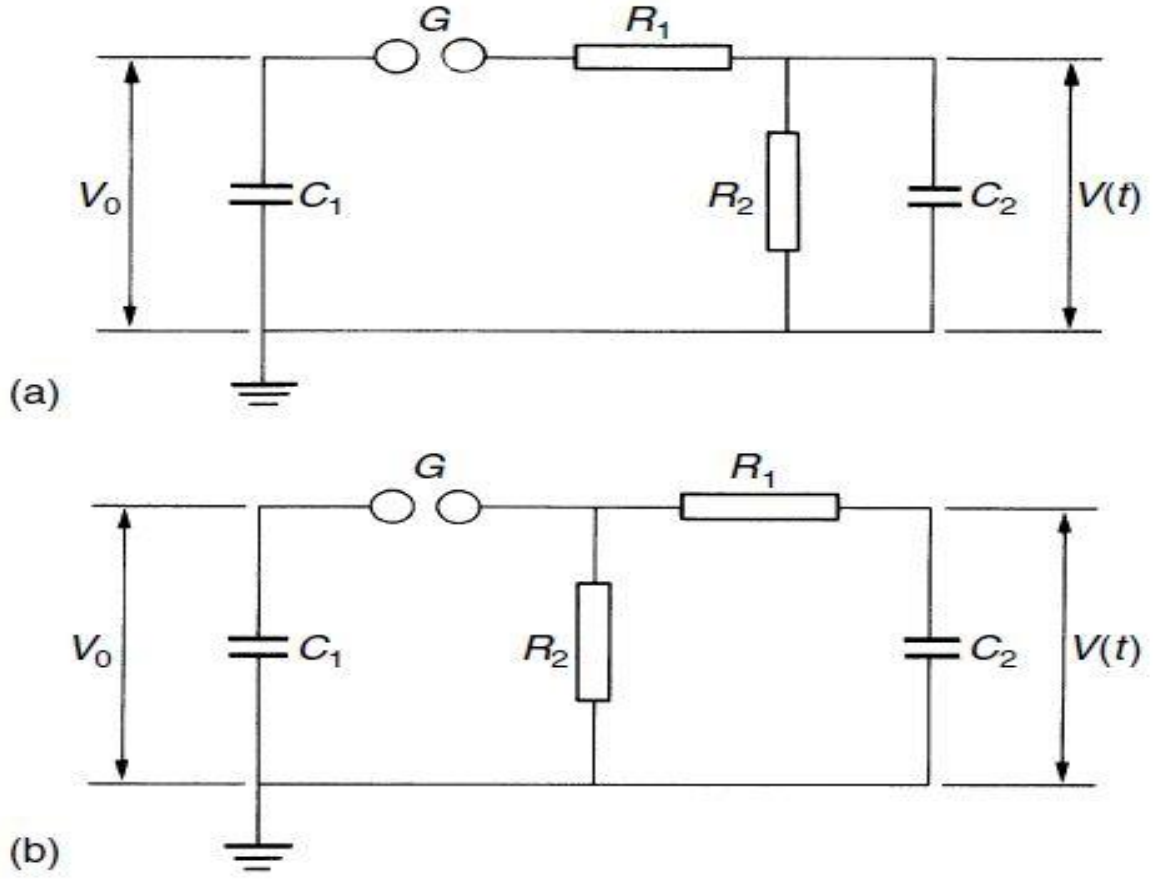

Figure 3.3*Single-stage impulse generator circuits (a) and (b).* C*1: Discharge capacitance.* C*2: load capacitance.* R*1: front or damping Resistance.*R*2: discharge resistance*

Before starting the analysis, we should mention the most significant parameter of impulse generators. This is the maximum stored energy**.**

$$W=\frac{1}{2}C_1 Vo_{max} \quad (3.2.1)$$

Within the 'discharge' capacitance C1. As C1 is always much larger than C2,

this figure determines mainly the cost of a generator.

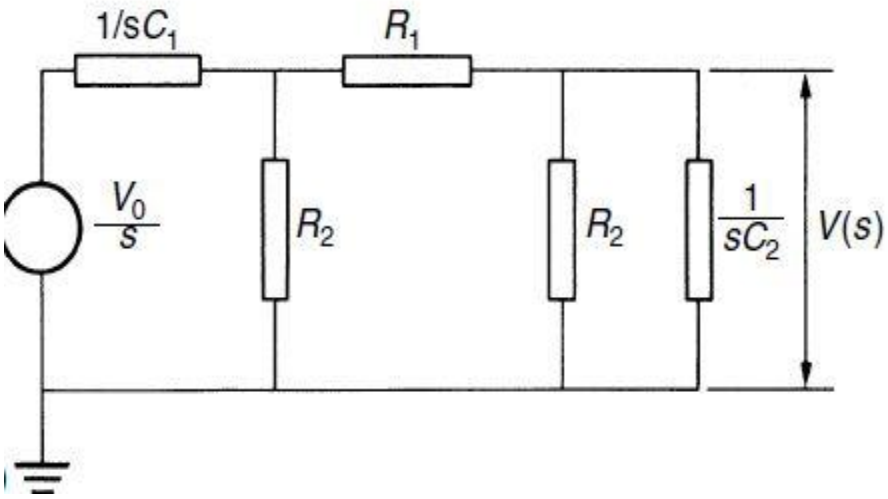

Figure 3.4 - Laplace equivalent circuit for double exponential

This circuit can be analyzed in the following manner.

$$\frac{V}{s} = i(s).\frac{1}{C_1 s} + i(s).R_1 + i_1(s).R_2$$

E(s)=$i_1(s).R_2$=$i_1(s).\frac{1}{C_2 s}$

Also, $i(s) = i_1(s) + i_2(s)$

$$i_1(s).\left(R_1 + R_2 + \frac{1}{C_1 s}\right) + i_2(s).\left(R_1 + \frac{1}{C_1 s}\right) = \frac{V}{s}$$

Also, $i_2(s) = C_2 R_2 \mathrm{s}.i_1(s)$

$$i_1(s).\left(R_1 + R_2 + \frac{1}{C_1 s} + R_1 C_2 R_2 \mathrm{s} + \frac{R_2 C_2}{C_1}\right) = \frac{V}{s}$$

Substituting gives,

$$E(s)=i_1(s).R_2 = \frac{VC_1R_2}{R_1R_2C_1C_2s^2+(R_2C_1+R_2C_2+R_1C_2)s+1}$$

If α, ß are the solution of the equation, $s^2 + as + b$

Where,

$$a= (\frac{1}{R_1C_1} + \frac{1}{R_1C_2} + \frac{1}{R_2C_1})$$

$$b= \frac{1}{R_1C_1R_2C_2}$$

Therefore, we obtain from the transform tables the same expression in the time domain:

$$E(s)=\frac{V}{R_1C_2}.\frac{1}{(s+\alpha).(s+ß)} = \frac{V}{R_1C_2}.\frac{1}{ß-\alpha}.[\frac{1}{(s+\alpha)} - \frac{1}{(s+ß)}]$$

That gives, $e(t)=\frac{V}{R_1C_2}.\frac{1}{ß-\alpha}(e^{-\alpha t}e^{-ßt})$ (3.2.2)

It is seen that the output waveform is of the double exponential form required.

The output voltage V(t) is therefore the superposition of two exponential functions of different signs. According to equation (3.2.2), the negative root leads to a larger time **constant 1/α** than the positive one, which is**1/ß**. A graph of the expression equation (3.2.2)) is shown in Fig. 3.5, and a comparison demonstrates the possibility to generate both types of impulse voltage switch these circuits.

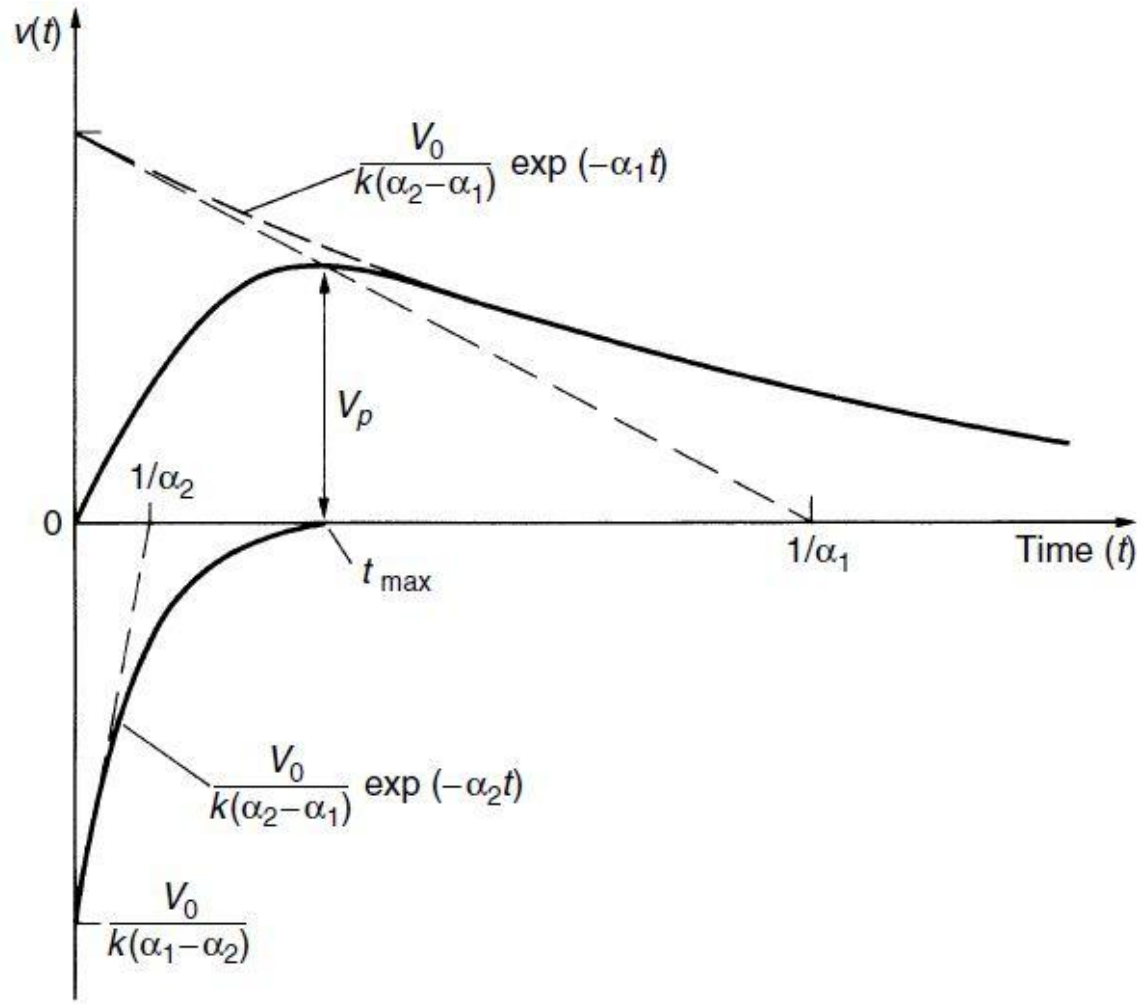

Figure 3.5 The impulse voltage wave and its components according to circuits in Fig. 3.3

All these equations contain the time constants 1/α and 1/ß which depend upon the wave shape. There is, however, no simple relationship between these time constants and the times T1, T2 and Tp as defined in the national or international recommendations, i.e. in Figs 3.3 and 3.4. This relationship can be found by applying the definitions to the analytical expression for V(t) this means to equation (3.2.1). The relationship is irrational and must be computed numerically. The following table shows the result for some selected wave shapes:

T_1/T_2 (μs)	T_p/T_2 (μs)	$1/\alpha_1$ (μs)	$1/\alpha_2$ (μs)
1.2/5	–	3.48	0.80
1.2/50	–	68.2	0.405
1.2/200	–	284	0.381
250/2500	–	2877	104
–	250/2500	3155	62.5

3.3 Standard Marx Impulse generator circuit

3.3.1 Single Stage Standard Marx impulse Circuit:

The energy storage capacitor, C1, is charged from the high voltage direct current (HVDC) power supply. The output waveform is controlled by the interaction of the front resistor R1 and the tail resistor R2 with the energy storage capacitor C1 and the load C2. The sphere gap in the circuit is a voltage limiting or voltage sensitive switch. Capacitor C1 charges from a dc source until the sphere gap breaks down. The time of breaking down of sphere gap is very short.

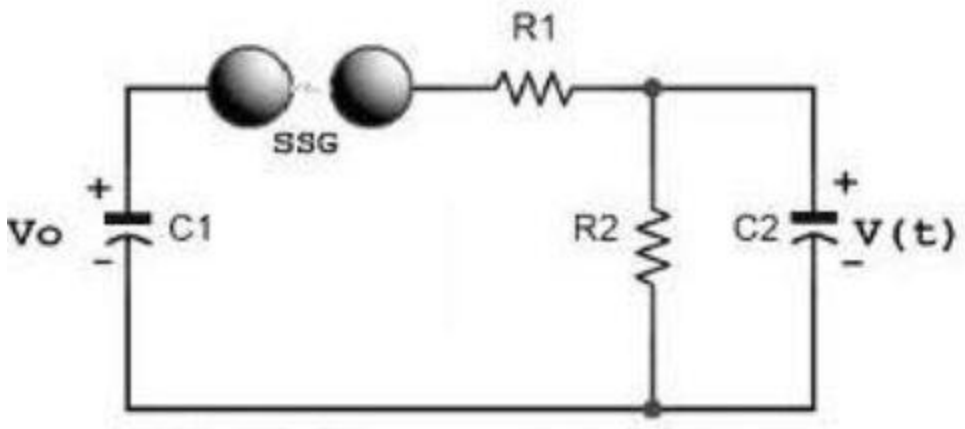

Figure 3.6: Single Stage Impulse Generator Circuit (Standard Marx circuit)

Charging voltage in large impulse generator can be of the order of mega volt (MV). The wave shaping network in the impulse generator consists of R1, R2 and C1. Resistor R1 basically damps the circuit and regulates the front time while R2 is the discharging resistor through which C1 will discharge. C2 is the load which represents the capacitance of the load itself and capacitance of other elements parallel with the load. Capacitor C1 discharges into the circuit comprising of R1, R2 and C2, when break down of the sphere gap takes place [5].Usually the impulse generator incorporates a load capacitance which is adequately large that the output waveform shape does not change considerably with changes in sample capacitance. The resistors R1, R2 and the capacitance C2 form the wave shaping network. R1 will primarily damp the circuit and control the front time T1. R2 will discharge the capacitors and therefore essentially control the wave tail. The capacitance C2 represents the full load, i.e. the object under test as well as all other capacitive elements which are in parallel to the test object [12], [13].Fast impulse or slower impulses can be generated if switching modifications are applied in theimpulse generating circuits. One probable way of generating longer pulse is to add an inductance in series with R1 [12], [14]. The difference in circuit arrangement will have different efficiency for the impulse generator. The dc voltage can be generated by the use of rectifier circuits. The rectifier used in the simulation is full wave rectifier circuit. The smoothness of dc

valueis not much of concern as it has to only charge the capacitor to peak. A sphere gap is a switch and the voltage across the sphere gap builds up as a voltage building up across capacitor takes place. Normally the sphere gaps are allowed to fire naturally or for smooth operation it can be fired through control methods.

3.3.2 Multi Stage Standard Marx impulse Circuit:

The multi-stage impulse generator uses several capacitors charged in parallel. These capacitors are then discharged in series to achieve higher voltages from a relatively low voltage source. The capacitors are discharged by use of spheres, which act as switches. This design was credited to E. Marx in 1924[15].As a result; the multi-stage generator is commonly referred to as a Marx generator.The operation of the multi-stage generator can be described as follows. All capacitors, one in each stage, are charged to a voltage V relative to ground. The bottom sphere gap is triggered by voltage injection and breaks down, discharging that stage capacitor. Subsequently, the remaining stage gaps also break down, discharging each stage capacitor. The result is a cumulative swing in voltage from zero to nV, where n is the number of stages in the Marx generator. The impulse generator used in this research is a three-stage unit capable of 300kV peak.

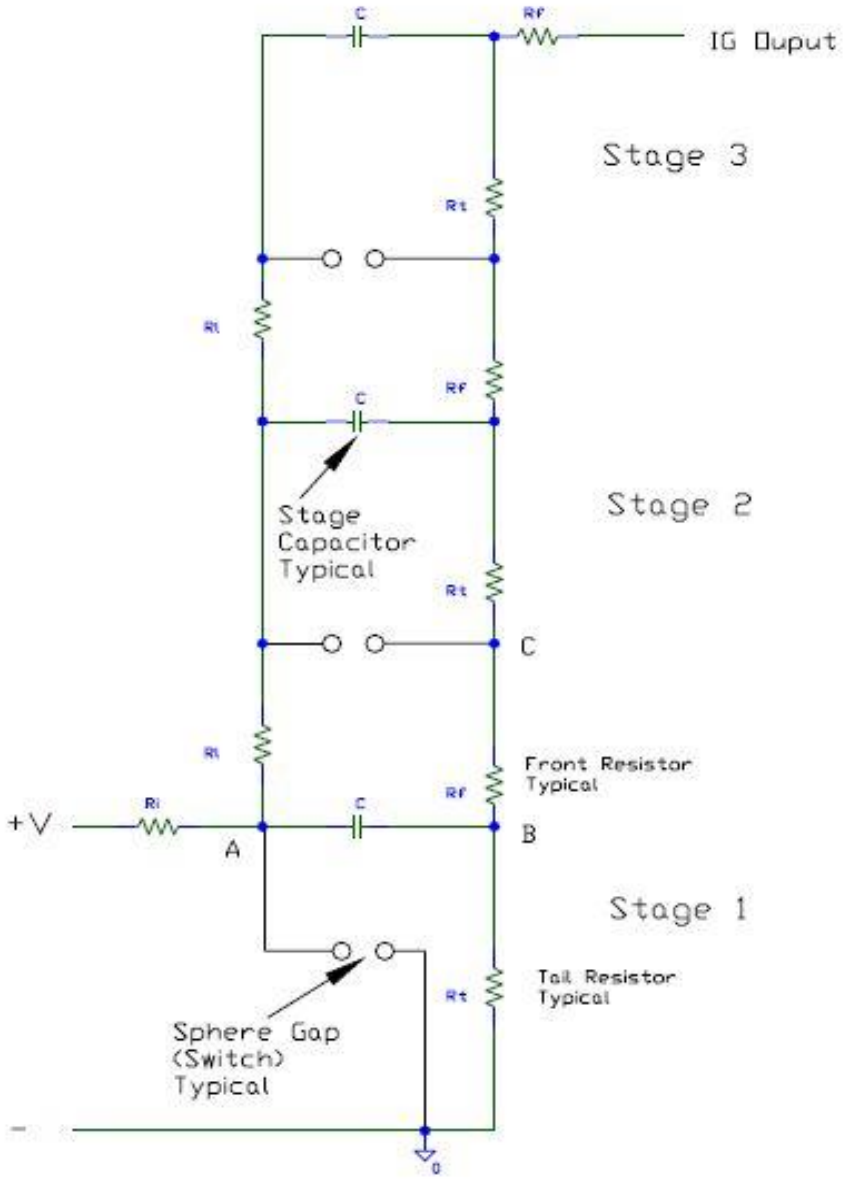

Figure 3.7 Multi Stage Marx Generator

capacitor is large enough to overcome the effects of the stray capacitance to allow the simultaneous gap breakdowns to occur [16].

Resistive Voltage Dividers

The voltage divider is used to reduce the level of the voltage to a measurable value and generally consists The sphere gaps act as switches. Once the first gap breaks down, the capacitor swings from V to zero, see point A Figure 2.6. This represents a swing of potential of –

V and at this instant the voltage at point C is -V. This results in a potential difference of 2V across the second gap and causing it to break down. This action continues across each stage gap. The first stage sphere gap, in effect, is a trigger for applying the peak voltage to the load. As part of the impulse generator, the load of two impedances in series. The two impedances result in a fraction of the total voltage across the lower leg impedance. The lower value impedance normally referred to as the lower leg, will have a voltage that is the input to the measurement instrument.

3.4 Calculation of Front time, Tail time

3.4.1 Calculation of α and ß from resistance and capacitance value:

Consider again the expression for the surge voltage

$e(t)=\frac{V}{R_1 C_2}.\frac{1}{ß-\alpha}(e^{-\alpha t}e^{-ßt})$

The peak value of this voltage occurs when its derivative becomes zero.

$\frac{de(t)}{dt}=0$; giving $\alpha e^{-\alpha t}= ß e^{-ßt}$

As, ß>>α so , $e^{(ß-\alpha)t}=\frac{ß}{\alpha} \approx e^{ßt}$ (3.4.1)

Maximum value of voltage is $E_{max}=\frac{V}{C_2 R_1}.\frac{1}{ß-\alpha}.(1-\alpha-\frac{\alpha}{ß})$

After reaching the peak, the voltage falls to half maximum in time t2 given by

$\frac{V}{2ßC_2 R_1}=\frac{V}{C_2 R_1 ß}.e^{-\alpha t}2$; $e^{-ßt}2<<e^{-\alpha t}2$

$\therefore e^{-\alpha t}2 \approx \frac{1}{2}$ (3.4.2)

From equations (2.4.1) and (2.4.2) it is seen that the wave front time [t1] is determined predominantly by β and the wave tail time is predominated by α .

$$C_1 C_2 R_f R_t s^2 + s(R_t C_1 + R_t C_2 + R_f C_2) + 1 = 0$$

$$\alpha * \beta = \frac{1}{C_1 C_2 R_f R_t}$$

$$\alpha + \beta = \frac{R_t C_1 + R_t C_2 + R_f C_2}{C_1 C_2 R_f R_t} \approx \beta; \beta >> \alpha$$

$$\alpha = \frac{1}{R_t C_1 + R_t C_2 + R_f C_2}$$

$$Generally, R_f << R_t$$

$$\beta \approx \frac{C_1 + C_2}{C_1 C_2 R_f}$$

$$\alpha \approx \frac{1}{R_t (C_1 + C_2)}$$

3.4.2 Definition of Wave front and Wave tail times of practical waveforms:

In practical impulse waveforms, the initial region and near the peak in the voltage are not very well defined. Also, near zero and near the peak, the rate of change is quite often much less than in the rest of the wavefront.Hence the wave front time is not well defined. It is thus usual to define the wave front by extrapolation based on a rise time for a specific change (say 10% to 90% or in even from 30% to 90% when the initial region is not clear). Figure 8.8 shows how the measurement of this rise time is made. Regarding the consideration, 8% to 86% is measured.

The wave front time is given as (t3 - t1)/ (0.9 - 0.1) or 1.25 (t3 - t1) for the 10% to 90% measurement and as (t3 - t2)/ (0.9 - 0.3) or 1.67 (t3 - t2) for the 30% to 90% measurement. The wave tail time is defined as the time from the initial point of the waveform to falling to 50 % of peak. In the case where the initial point is not well defined, the initial point may be extrapolated from the wave front.

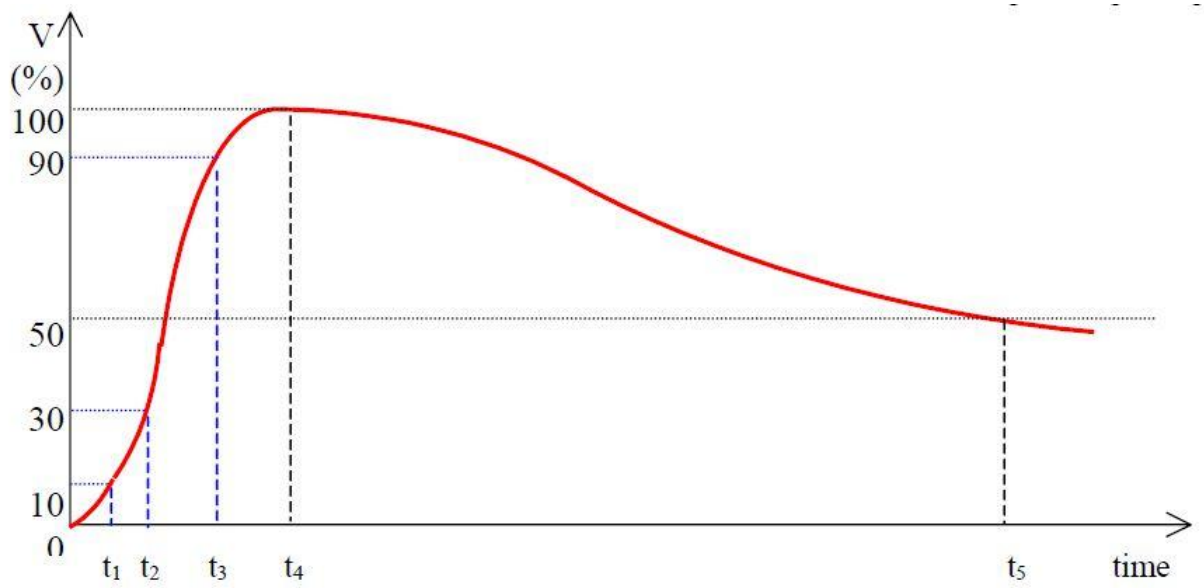

Figure 3.8 Definition of wave front

In a practical impulse generator circuit, the nominal voltage is defined by the peak theoretical voltage and the nominal energy is defined by the maximum stored energy. The capacitance values in the impulse generator circuit are not variable except for the capacitance contribution of the test object. Thus wave shape control is achieved by varying the resistance values.

The wave front time, (t_f) :

Defining the wave front from 8 % to 86 % and considering only that β determines wave front,

$$t_f = \frac{t_b - t_a}{0.9 - 0.1} = 1.28(t_b - t_a)$$

$$1 - 0.8 = e^{-\beta t_a}, 1 - 0.86 = e^{-\beta t_b}$$

$$t_a = -\frac{1}{\beta}\log_e(0.92) = \frac{.0833}{\beta}$$

$$t_b = -\frac{1}{\beta}\log_e(0.14) = \frac{2.0402}{\beta}$$

(3.4.3)

The wave tail time,(t_t):

Similarly, defining the wave tail time as the time to decay to 45 % of peak, and considering only α that determines the wave tail,

$$0.55 = e^{-\alpha t_t}$$

$$\alpha = -\frac{\log_e(0.55)}{t_t}$$

(3.4.4)

$$t_t = \frac{.598}{\alpha}$$

3.4.3 Analyzing the circuit with voltage divider (For n stages)

The standardized nominal values of T1 and T2 are difficult to achieve in practice, as even for fixed values of C1 the load C2 will vary and the exact values for R1 and R2 are in general not available. These resistors have to be dimensioned for the rated high voltage of the generator and are accordingly expensive. The permissible tolerances for T1 and T2 are therefore necessary and used to graduate the resistor values. A recording of the real output voltage V(t) will in addition be necessary if the admissible impulse shape has to be testified. Another reason for such a measurement is related to the value of the test voltage .This magnitude corresponds to the crest value, if the shape of the lightning impulse is smooth. However, oscillations or an overshoot may occur at the crest of the impulse. If the frequency of such oscillations is not less than 0.5MHz or the duration of overshoot not over 1 μsec, a ‘mean curve’ (see Note below) should be drawn through the curve. The maximum amplitude of this ‘mean curve’ defines the value of the test voltage. Such a correction is only tolerated, provided their single peak amplitude is not larger than 5 per cent of the crest value. Oscillationson the front of the impulse (below 50 per cent of the crest value) aretolerated, provided their single peak amplitude does not exceed 25 per centof the crest value. It should be emphasized that these tolerances constitute thepermitted differences

between specified values and those actually recorded bymeasurements. Due to measuring errors the true values and the recorded onesmaybe somewhat different. The voltage divider is used to reduce the level of the voltage to a measurable value and generally consists of two impedances in series. The two impedances result in a fraction of the total voltage across the lower leg impedance. The lower value impedance normally referred to as the lower leg, will have a voltage that is the input to the measurement instrument.

After analyzing with voltage divider,

(3.4.5)
$$\beta = \frac{\frac{C_1}{n} + C_2}{n(R_f + R_t)\frac{C_1}{n}C_2}$$

(3.4.6)
$$\alpha = \frac{1}{(\frac{C_1}{n} + C_2) * (\frac{R_d * R_d}{R_d + R_d})}$$

3.5 Schematic Diagram in Pspice

The Multi-stage impulse generator was simulated using PSPICE™ software. The schematic of the simulated generator for firststages is shown in Figure 2.8. The stage sphere gaps were simulated by the use of switches, as shown. The output of the generator was also switched, and all four switches were closed at the same time. Each of the three stage capacitors were given an initial charge voltage value, which is equal to 1/3 of the total kV test voltage. The values of front and tail resistors, as well as the stage capacitors, are the same as used in the mathematical model of the impulse generator. The basic circuit used for generation of impulse wave is shown in Figure 2.8. The sphere gap in the circuit is a voltage limiting or voltage sensitive switch. Capacitor C1 charges from a dc source until the sphere gap breaks down. The time of breaking down of sphere gap is very short. Charging voltage in large impulse generator can be of the order of mega volt (MV). The wave shaping network in the impulse generator consists of R1, R2 and C1. Resistor R1 basically damps the circuit and regulates the front time while R2 is the

discharging resistor through which C1 will discharge. C2 is the load which represents the capacitance of the load itself and capacitance of other elements parallel with the load. Capacitor C1 discharges into the circuit comprising of R1, R2 and C2, when break down of the sphere gap takes place.

The circuit setup for simulation of first stage of Standard Impulse Generator is shown below:

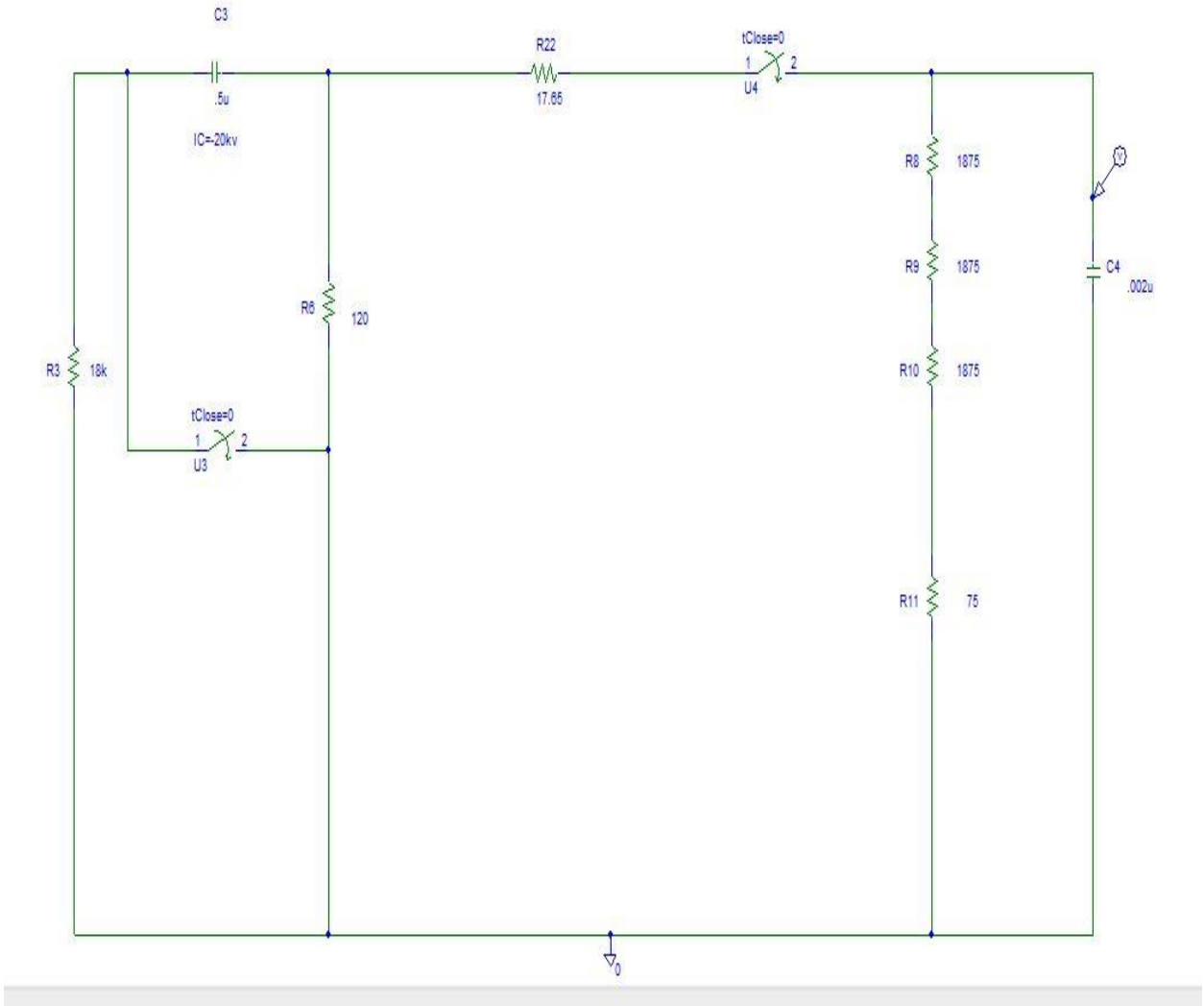

Figure 3.9*Schematic Diagram of Single Stage Standard Marx Impulse Voltage Generator*

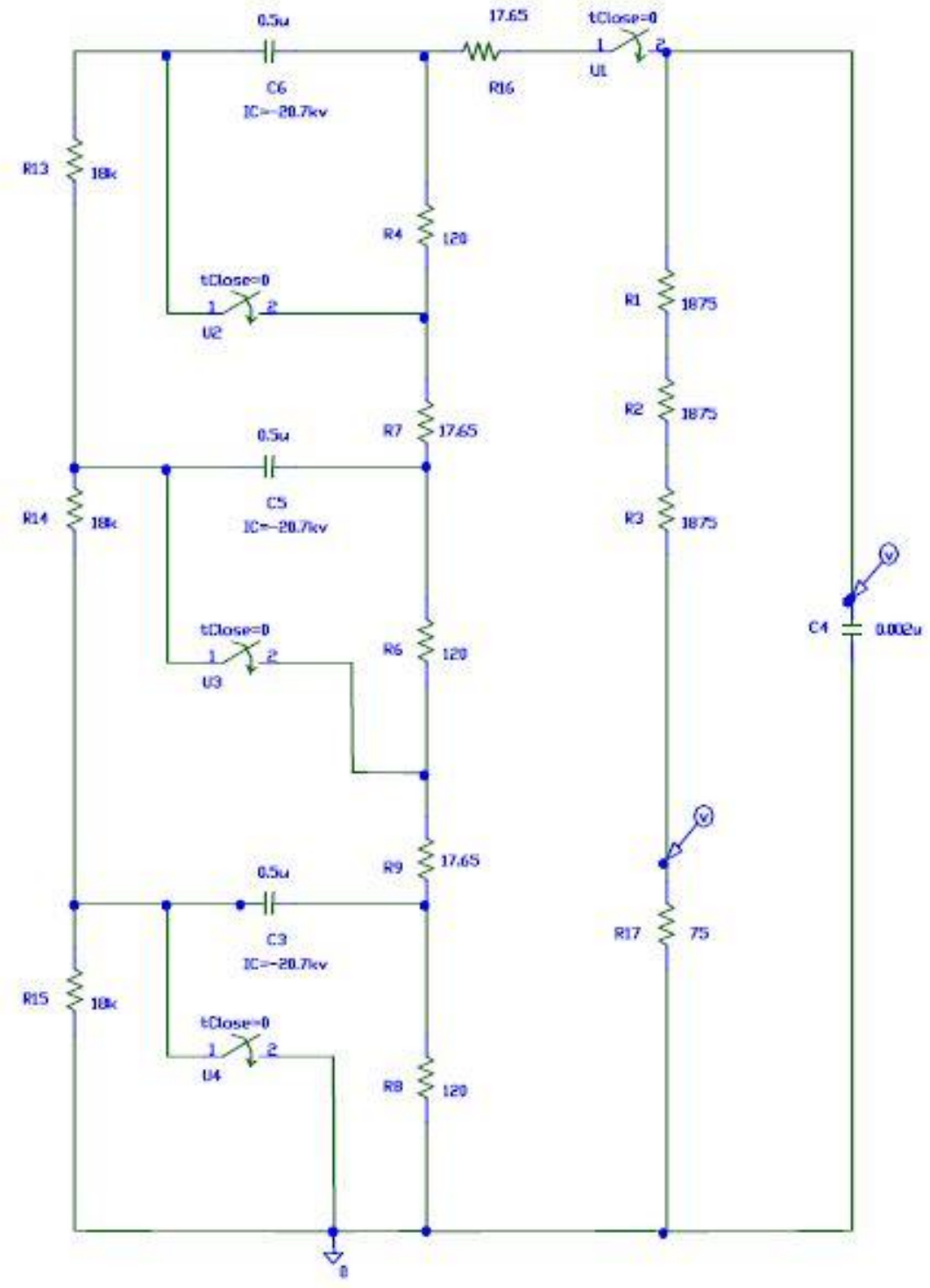

Figure 3.10 Schematic Diagram of 3rd Stage Standard Marx Impulse Voltage Generator

Standard impulse wave for the first stage using the Standard Marx Impulse generator is shown below.

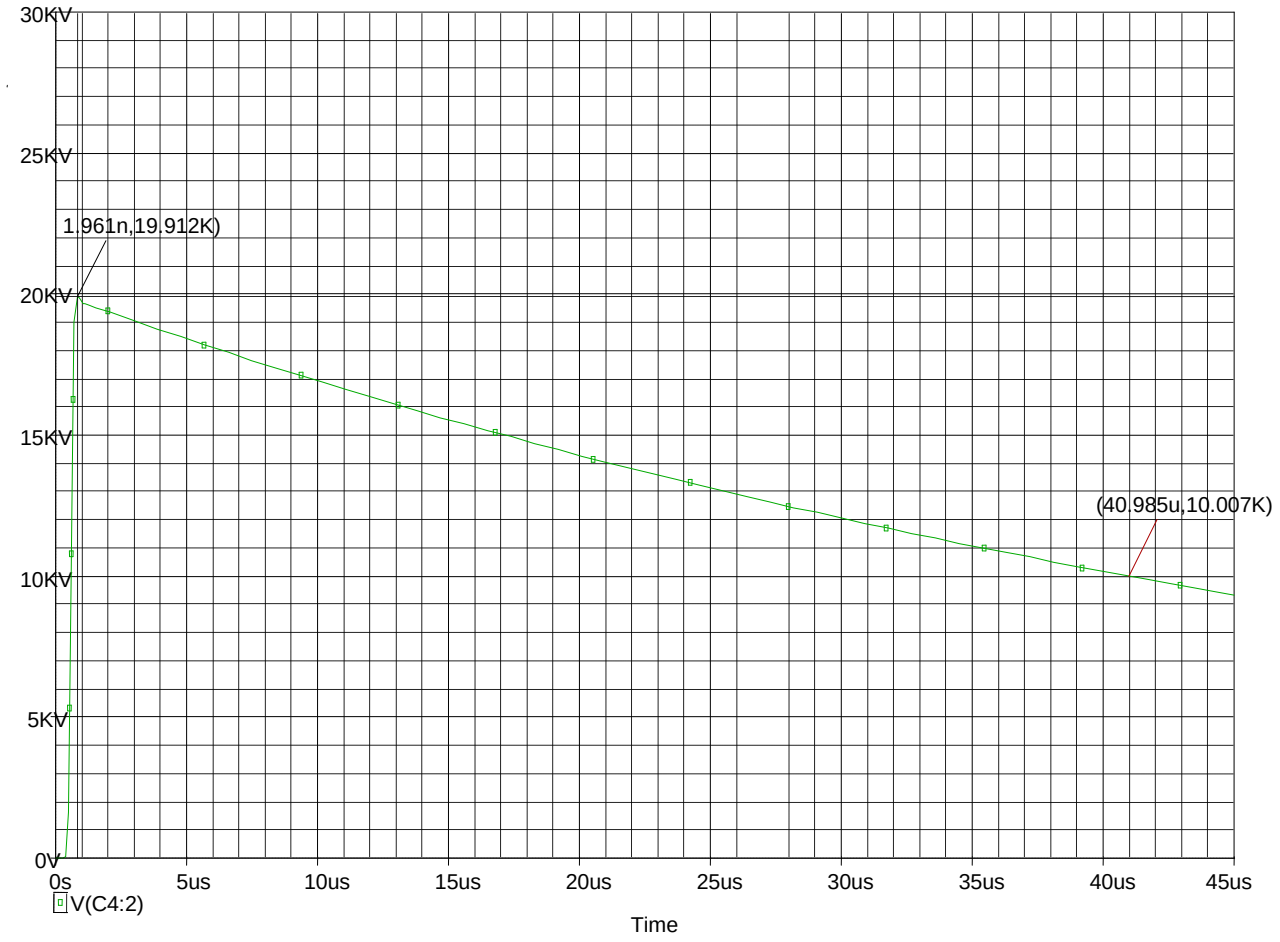

Figure 3.11 A standard impulse wave (stage 1 using Standard Marx impulse voltage circuit)

In the first stage the dc charging voltage supplied was around 20kV and as shown in the Figure 2.9 the Marx Impulse Generator produces an output impulse wave with a peak of 19.91kV. The

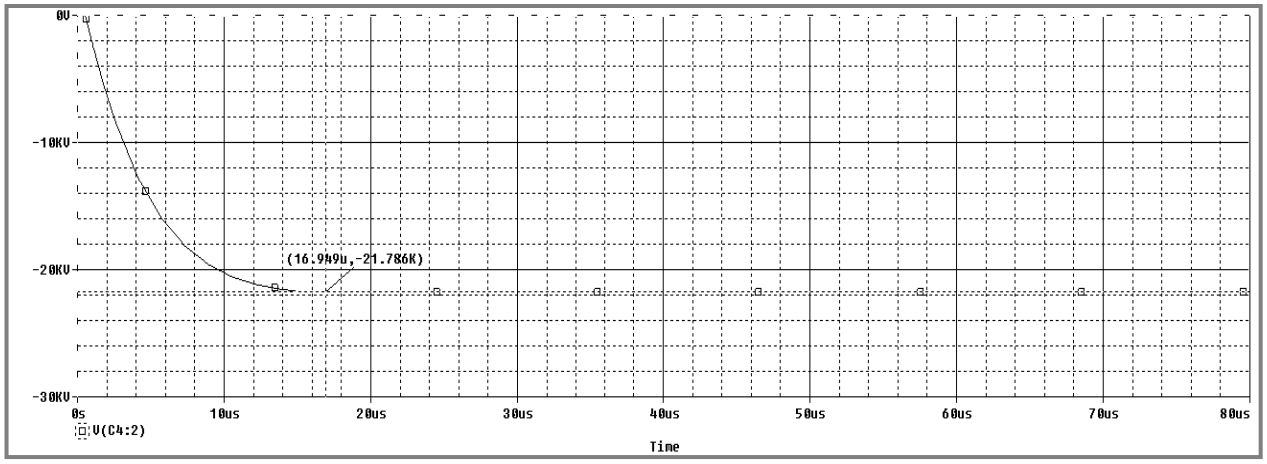

output value is obtained as a result of discharging of the fully charged capacitor through R1 and R2. The discharge phenomenon occurs when the switch is triggered. Now the output voltage is slightly less than the charging voltage which is acceptable

The output waveforms of second, third and fourth stage of Standard Marx impulse generator with their peaks indicated on the graph is shown below

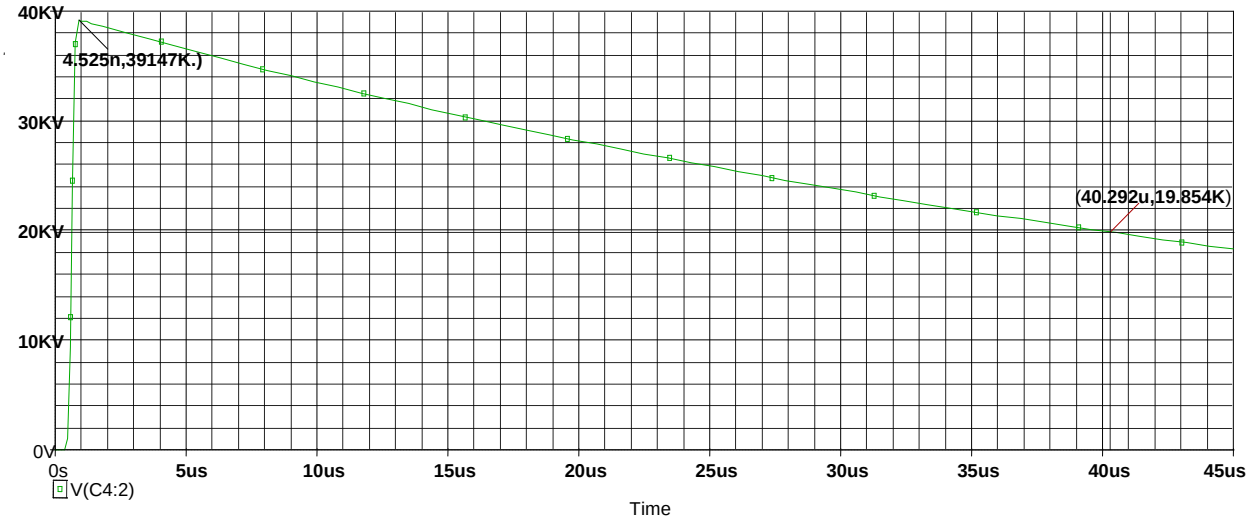

Figure 3.12A standard impulse wave (stage 2 using Standard Marx impulse voltage circuit)

60KV

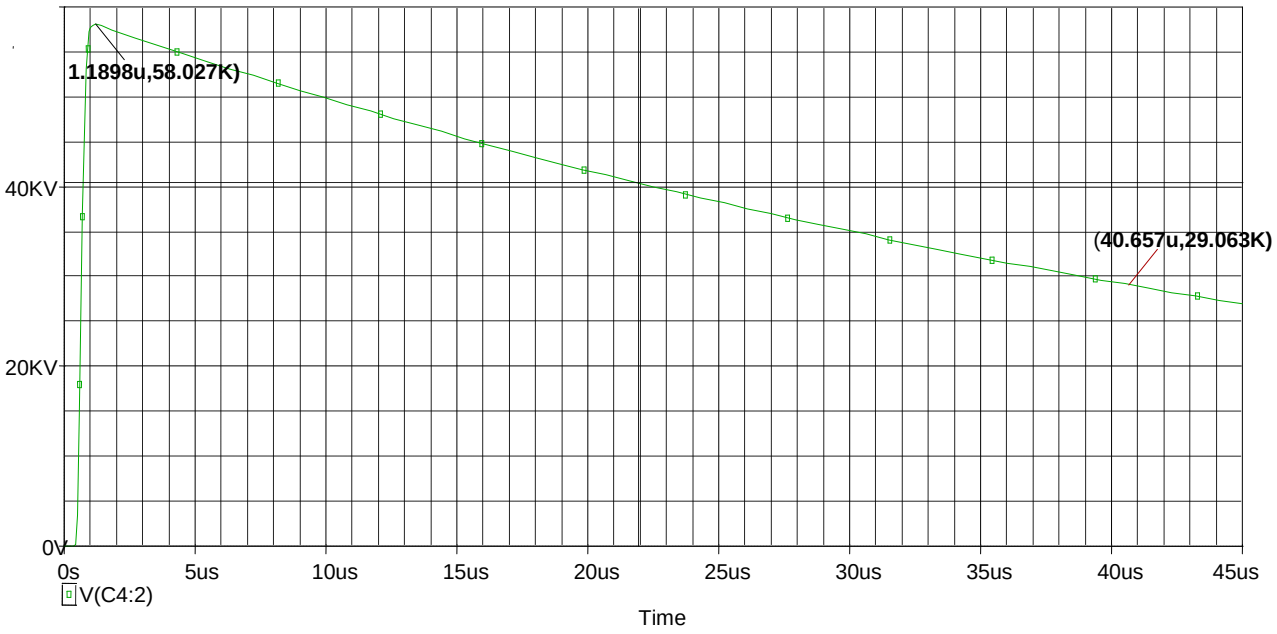

Figure 3.13A standard impulse wave (stage 3 using Standard Marx impulse voltage circuit)

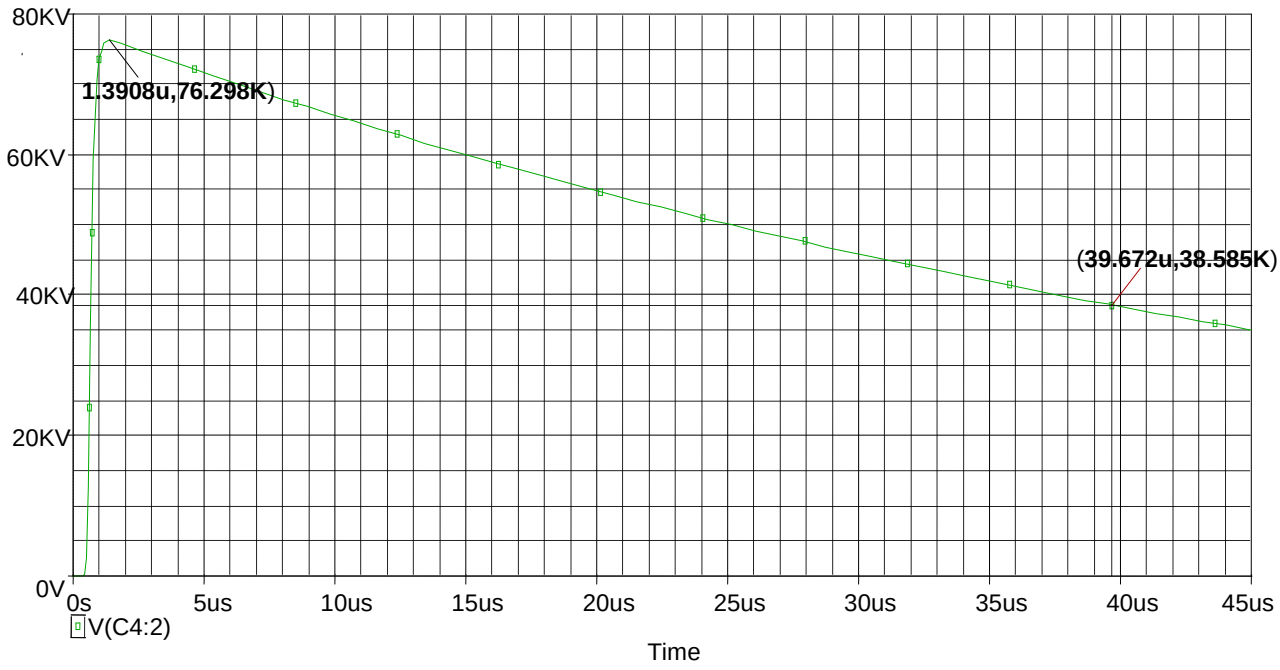

Figure 3.14A standard impulse wave (stage 4 using Standard Marx impulse voltage circuit)

3.6 Result Analysis

Rise time is 1.28 times of difference between the time taken to reach 86% of peak impulse voltage and time taken to reach 8% of peak impulse voltage. Similarly, tail time is the difference between the time taken to reach 50% of peak impulse voltage during discharging and time taken to reach 10% of peak impulse voltage during charging. The front time, tail time and peak voltage calculated for all the 4 stages have been formulated below in a table below.

For a standard impulse wave the front time is 1.2μ sec and tail time is 50μ sec and the allowable percentage of error for rise and fall time is 30% and 20%. The front time, tail time and error for the observed results has been tabulated.

To obtain the values of impulse voltage at 10%, 90% and 50% cursor option in the toolbar of Pspice software is used. To use it first the peak value is recorded and according to that its 8%, 86% is calculated. Then by putting these values the corresponding values on time axis is shown on the graph.

The values of front time, tail time and error in front time and tail time were calculated following the (3.4.3),(3.4.4),(3.4.5),(3.4.6)equations. These values were calculated for a total of four stages and were tabulated. The table for front time, tail time and error calculation is shown below. The same values of resister are capacitors are used in simulation and mathematical model.

Front Time and Error Calculation (Theoretical and mathematical): Table-1

Stage		**Mathematical**	**Simulation**	**%Error**	
1.	3.17	.76us	.83us	9.2%	19.91k

2.	1.83	1.3us	.92us	29%	39.14k
3.	1.22	1.96us	1.2us	38%	58.02k
4.	.97	2.3us	1.3us	43%	76.29k

As described above the percentage of error is quite high, because the comparison is done between the tolerance considered mathematical model and the exact front time.

Tail Time and Error Calculation (Theoretical and mathematical): Table -2

Stage	α	**Mathematical** $t_t = \frac{.693}{\alpha}$	**Simulation**	**%error**
1.	**.0167**	**41.49us**	**40.8us**	**1.6%**
2.	**.017**	**40.76**	**40.07us**	**1.6%**
3.	**.0127**	**55us**	**40.6us**	**2.46%**
4.	**.016**	**43.5us**	**39.69us**	**8.7%**

Efficiency calculation: table -3

Stage	V_p(Volts)	Efficiency %
1.	19.91	99%
2.	39.14	97.85%
3.	58.3	97%
4.	76.3	95.3%

A small scale of generation of high impulse voltage is implemented in the simulation with thePspice Software environment. It is found that the overall simulated result is close to standard impulse generator 1.2 / 50 μs wave shape for all the stages of Marx generator. The ratio of C1/C2 is taken as 20 in each stage and the impulse waveform was governed by the values of front resistor and tail resistor. The energy and efficiency at each step was calculated and was tabulated. For simulation the sphere gap is replaced with a simple switch in Pspice Software.

The values from mathematical model and simulated waveforms in the fields of rise time, tail time, peak voltage and error in rise time and tail time have a considerable amount of difference Shown in Table 1,2,3. As explained above, the difference is caused by a number of factors. The prime reason is the difference in the chargingresistors and capacitors used in the simulation and practical circuit. The tolerances level of resistors used in practical circuit are different from those used inPspice and the maximum charging voltages in both practical and simulation aren't the same. Moreover the connection of resistors and capacitors in parallel and series gives an approximate value of what is exactly used in simulation also adds to the errors. Due to these parameters differences have resulted in the two circuits. In practice all the capacitors are not charged to the same value due to the presence of series resistance in the circuit as the series resistance between the source and distant capacitor limits the voltage obtainable.

In this work, the entire circuit is modeled, simulated designed in the impulse Marx circuit. The effects of the circuit parameters on the impulse wave characteristics is also studied and it is found that as long as the proper parameter selection is made the circuit will produce the standard waveform from the Standard as well as Improved Marx Impulse voltage generator.

CHAPTER 4

Simulation of Energy Storage System

4.1 Energy Storage

Due to extremely high energy density and power density, energy obtained from lightning cannot be directly fed to the grid. So, it is obvious, energy storage medium is indispensable. The transient time of a lightning is in the order of 100μs, where peak current becomes half within 50μs[4]. So, storage medium must be able to charge within this extremely short time. Though capacitors have limited energy density, they have fast charging and discharging ability. Following figure shows a comparative study among different power sources.

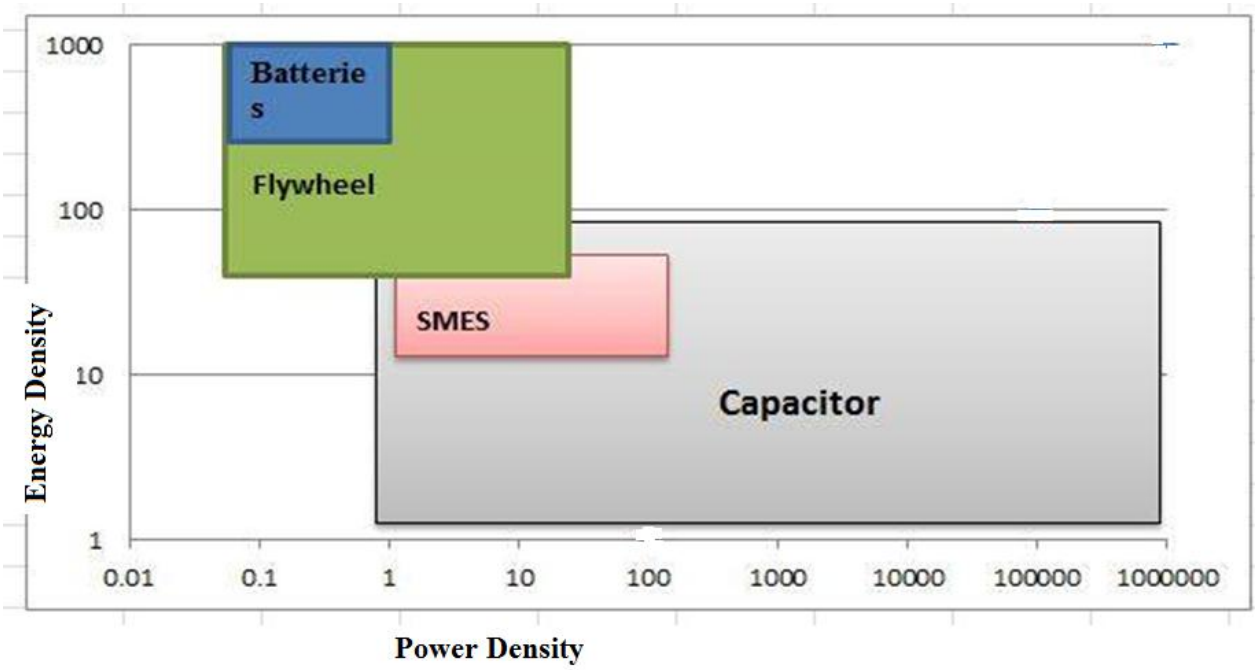

Figure4.1: specific energy ranges versus specific power [17]

Supercapacitors provide fast charging and discharging rate extra energy density compared to static capacitors. Other energy sources, like batteries have high energy density, but very slow charging and low power density. So, the study suggests that, capacitor is the preeminent alternative for energy storage medium. [17]

For the simulation purpose, CLASSX2 Metalized Polypropylene Film Capacitor is used, because of high Temperature Stability, readily Available, widely used in high frequency, pulse circuits and DC applications.

4.2High Speed Switching Circuit

According to the standard wave shape, peak Voltage occurs at 1.2us. So, the sample capacitor must be isolated just after 1.2us to prevent the capacitor to be discharged again. For this purpose, high speed switching circuit is used.[17]

Components used in high speed switching circuit are as follows -

1. Microcontroller: ATmega16

2. Gate drive circuitry: NPN transistor, relay, Rectifier, Resistor

3. Switching device: IGBT (IRG4PH50UD)

ATmega16 is renowned high-performance, Low-powerAVR microcontroller. It is an 8 bit microcontroller manufactured by Atmel.

Properties of ATmega16 are as follows-

1. Speed: 16MIPS at 16MHz clock input
2. 512 Bytes EEPROM
3. 1 Kbyte Internal SRAM
4. Operating Voltage 4.5V to 5.5V [18]

For this high speed switching circuit, two level of voltage supply needed. 20V is required at the gate to turn ON the IGBT, whilst 0V is required to turn OFF the IGBT.So, the gate gate drive consists of one NPN transistor and one relay. NPN transistor provides sufficient current to drive the relay, where relay drive the IGBT.

Rectifier is used to bypass the gate resistor of the IGBT when gate voltage is zero, so that, gate charges can be easily gone to the ground.

NPN transistor and Microcontroller required 5V dc, relay operating voltage is 20V dc.

Properties of IGBT (IRG4PH50UD)-

1. Collector to Emitter Breakdown Voltage (V_{CES}) = 1200V
2. Continuous Collector Current (I_C at T_C = 25°C) = 45A
3. Continuous Collector Current (I_C at T_C = 100°C) = 24A
4. Turn-Off Delay Time ($t_{d(on)}$) = 240ns at T_J = 25°C [19]

The IGBT has very little turn off time delay, it can. The peak voltage occurs at 1.2us where switching time delay is 0.24us. So, if the switch turn off time is set as t=1us, the overall switching time is 1.24us. After 1.24us, the Storage Capacitor will be isolated from the circuit. The voltage of the capacitor is thus remains constant, as there is no discharging path. Now the capacitor is like a battery, so it can be used as an energy source by connecting load with it. The

voltage level of the capacitor is now maintained constant, so, it is now going to be used for further inspection. [17]

Overall block diagram of the high speed switching circuit is as following.

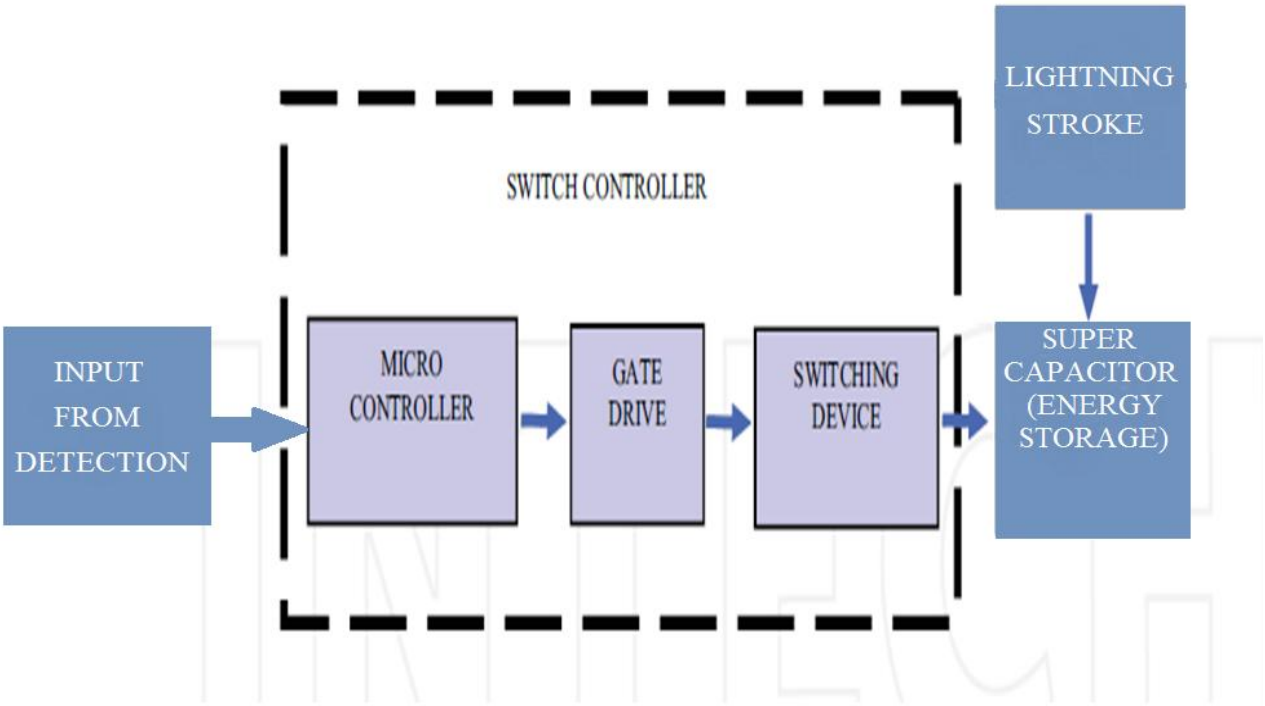

Figure4.2: Overall Block Diagram of the high speed switching circuit [18]

This circuit gets the input from detection part, and turn on the IGBT, and again turn off the IGBT after reached the peak voltage. As marx generator is used for mock lightning, in the simulation, input is manually set. The storage part simulation is done with the PSpice with additional switch added with marx generator to represent the IGBT, simulation output graph analysis is also done there.

But, in order to show the circuit configuration with microcontroller, gate drive, and IGBT, proteus is used to simulate the high speed switching circuit. With the help of PWLIN signal generator, mock lightning signal with low voltage magnitude is formed.

4.3 High Speed Switching Circuit Simulation

4.3.1The overall circuit diagram of the High Speed Switching Circuit

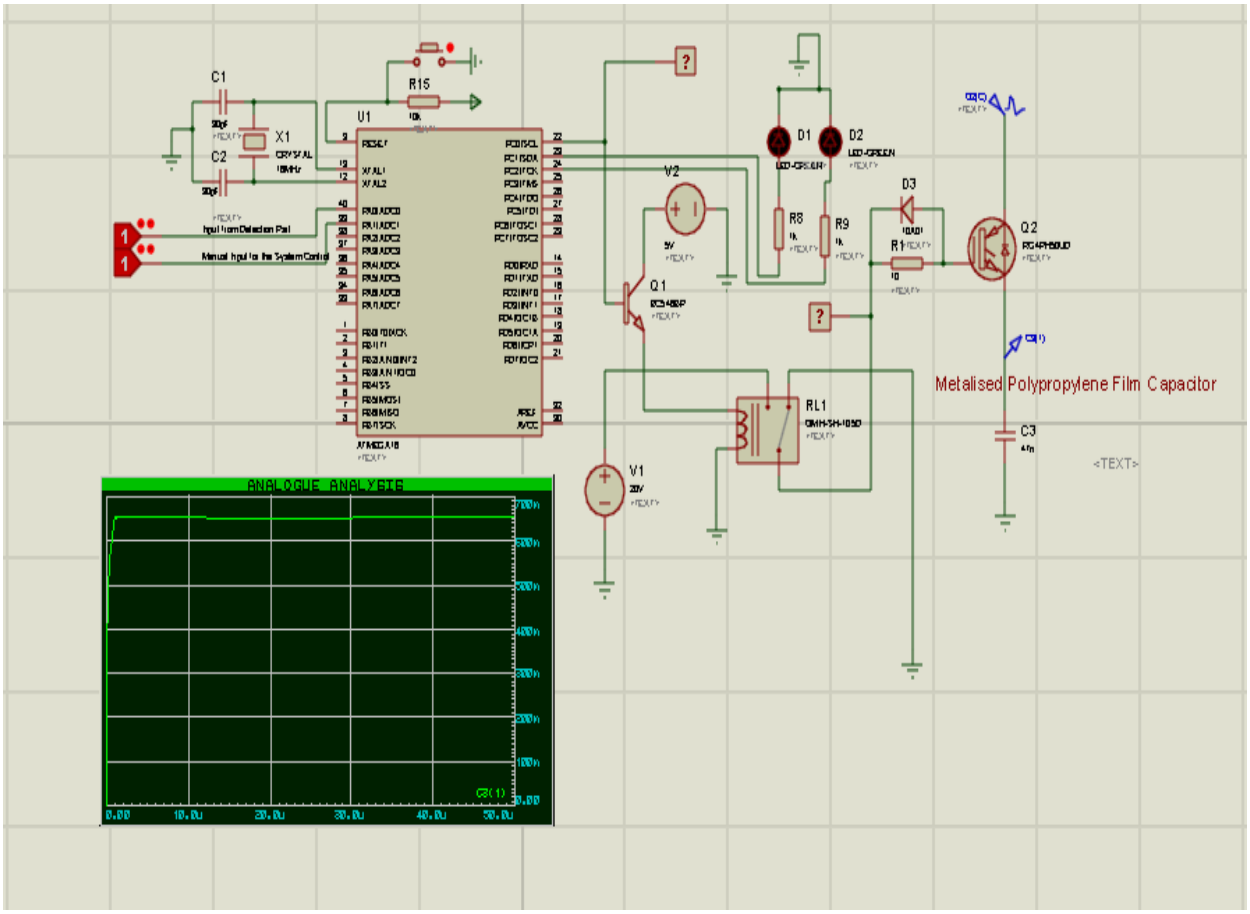

Figure4.3: Overall circuit diagram for high speed switching.

Two LED's are used to show the state, weather lightning hit or not, and the logical input for IGBT is high or low. 16MHz clock input is provided from the oscillator circuit. Two different sources, one 20V battery and another 5v battery is used to power up the circuit.

The time vs. voltage across the storage capacitor graph is contrived. This graph shows that, after reached the peak voltage, the voltage level of the storage capacitor is maintained constant.

4.3.2 Flowchart of the high speed switching circuit

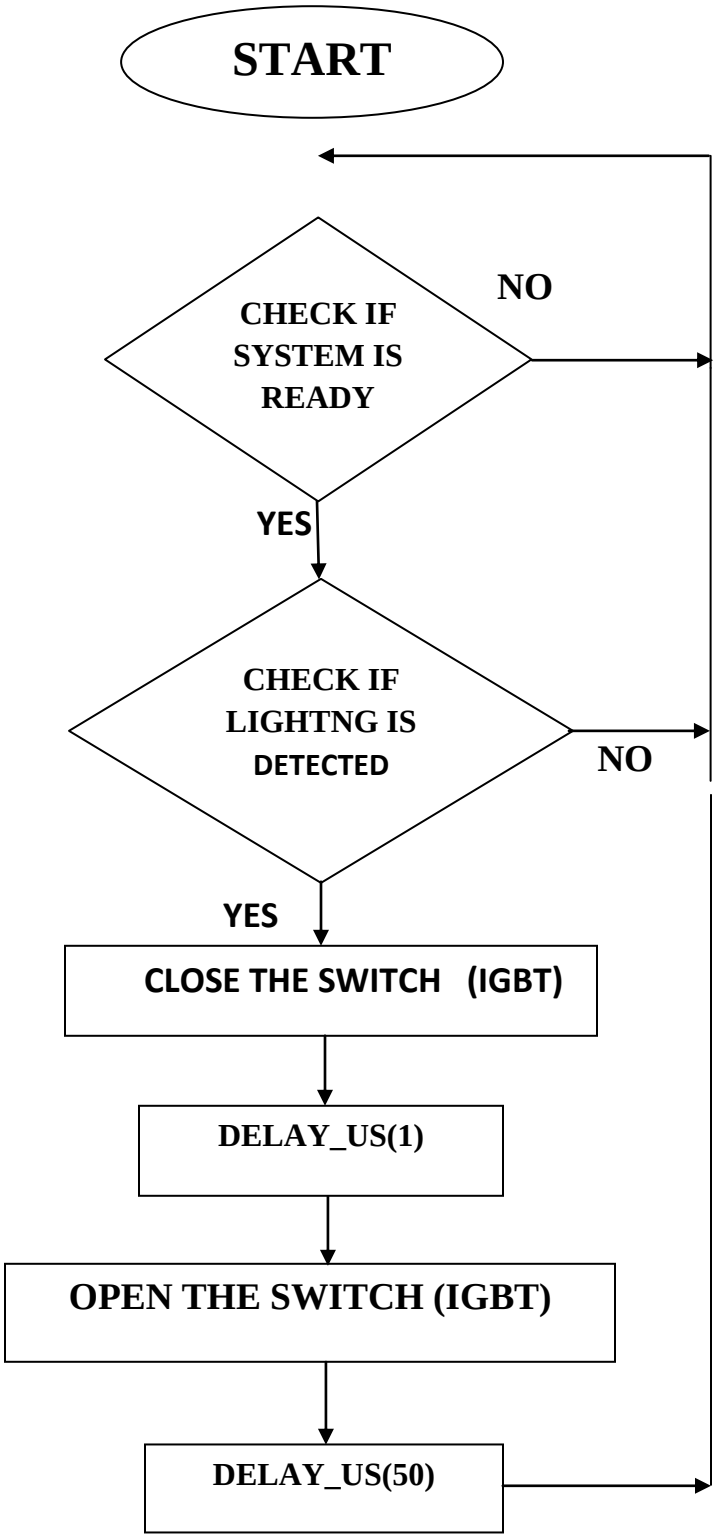

4.3.3 Coding of the high speed switching circuit

```
void main() {
```

```
DDRC=0XFF;
DDA0_bit=0;
DDA1_bit=0;
while(1){
if(PINA0_bit==1){
if(PINA1_bit==1){
    PORTC0_BIT=1;
    PORTC1_BIT=1;
    PORTC2_BIT=0;
delay_us(1);

    PORTC0_BIT=0;
    PORTC1_BIT=0;
    PORTC2_BIT=1;
delay_us(50);

  }
else{
    PORTC0_BIT=0;
    PORTC1_BIT=0;
    PORTC2_BIT=1;
delay_us(1);
   }
 }
```

```
else{
   PORTC0_BIT=0;
   PORTC1_BIT=0;
   PORTC2_BIT=1;
delay_us(1);
  }
  }
}
```

.

4.4 Simulation of the Storage Part with Additional Switch

In fig 4, the circuit shown is alike the marx generator circuit, except an additional normally close switch is used. This switch is representing the IGBT used in the high speed switching circuit simulation. Here, the simulation is done with PSpice. As peak voltage occurred within 1.2us, this

switch is set to open at t=1us. Switching transient is set to 0.24us, as the turn off delay of the IGBT is 240ns

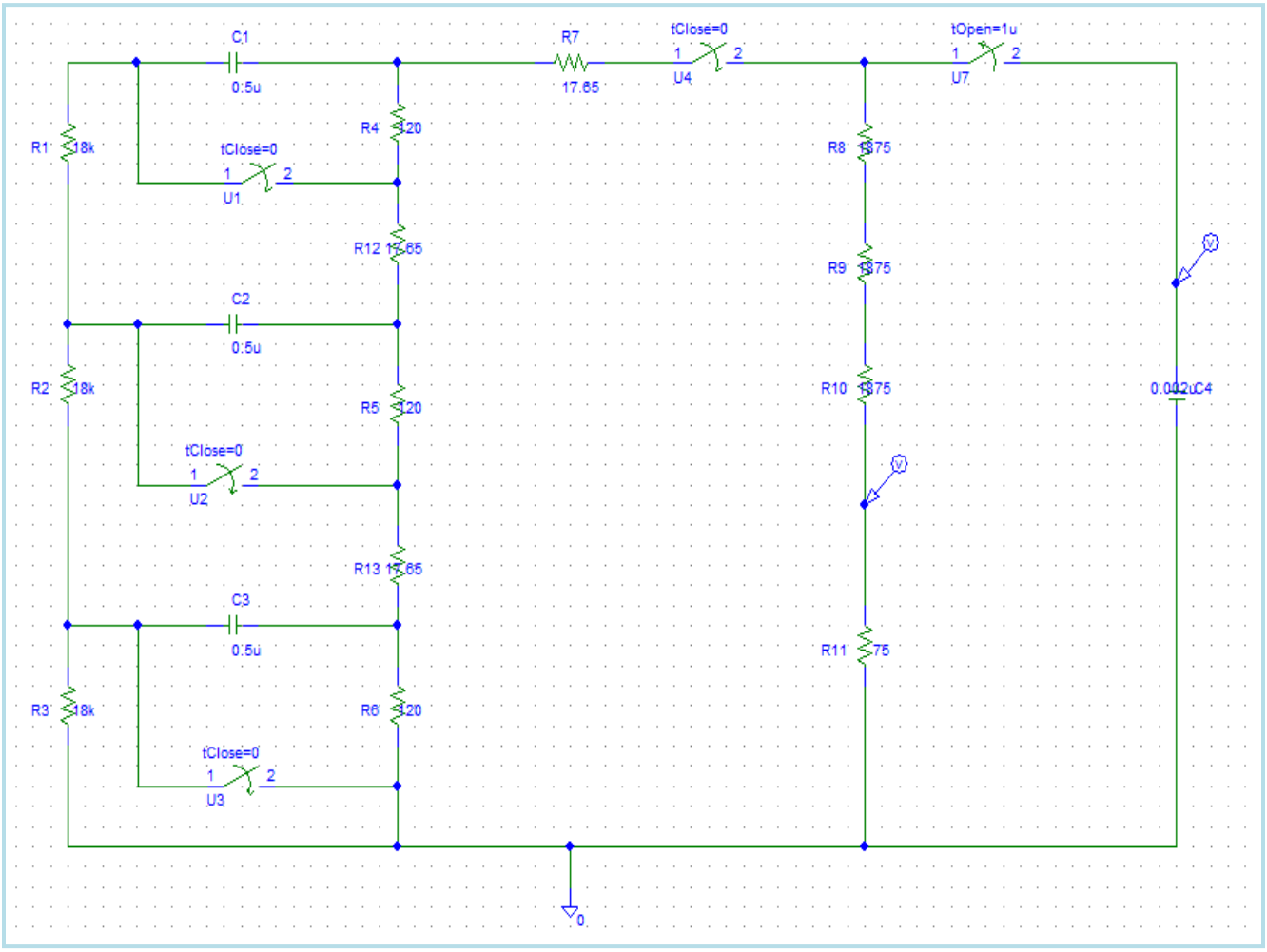

Figure4.41: Circuit with additional switch. Switch U7 is open at time t=1us

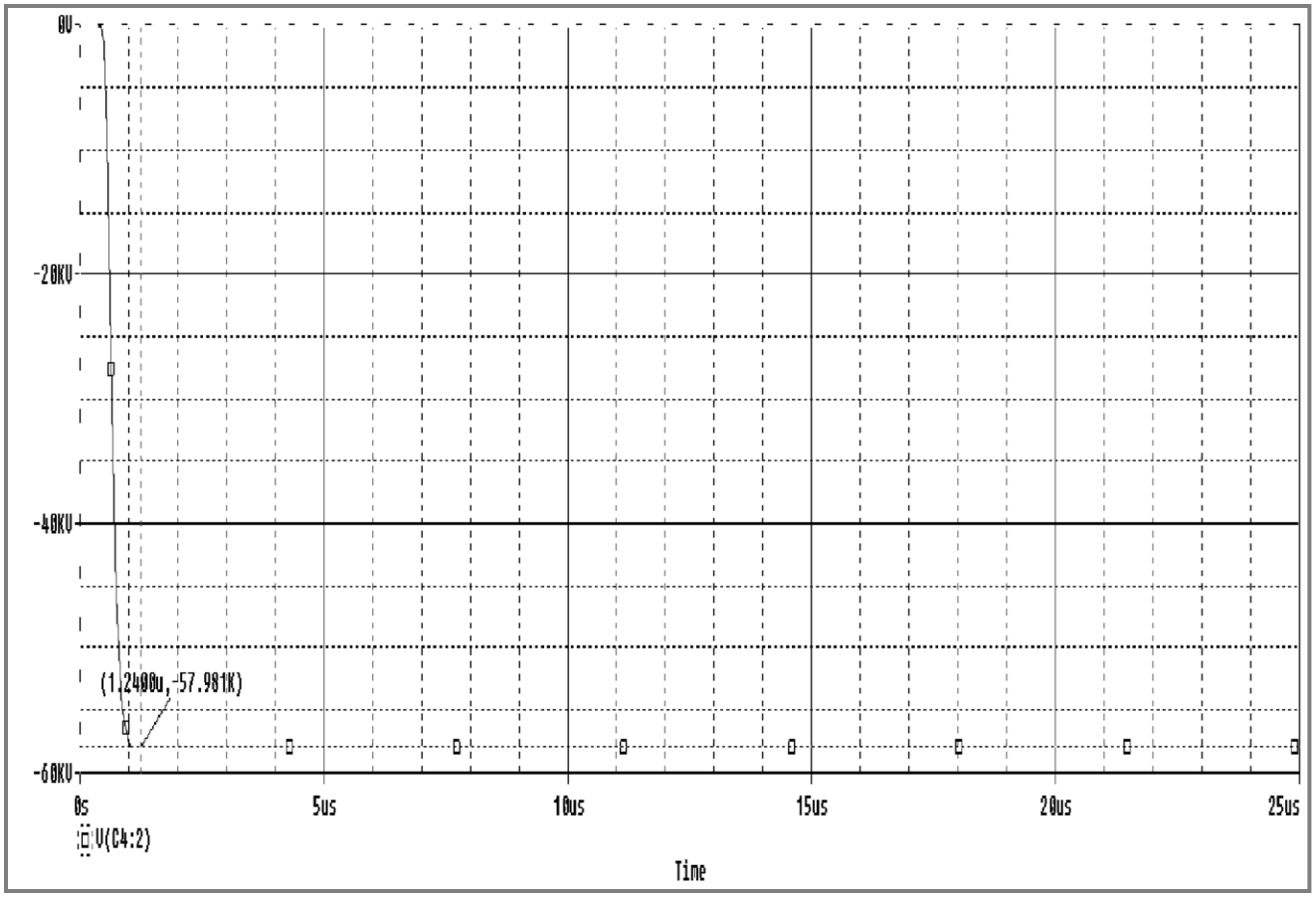

Figure4.42: Voltage vs. time graph from the Simulation of the circuit of fig 4

Denoting to the Figure above, the voltage of the load capacitor CB is not decaying after reach the peak value at 1.24μs. It demonstrates that, when the switch is applied in the circuit, the voltage is maintained constant. It illustrates that, the capacitor CB is not able to discharge because it is isolated from any connection.

4.5 Effect of changing Storage Capacitor Value

Following graphs are produced from replacing the storage capacitor with 0.22uF, 0.47uF and 0.68uF respectively.

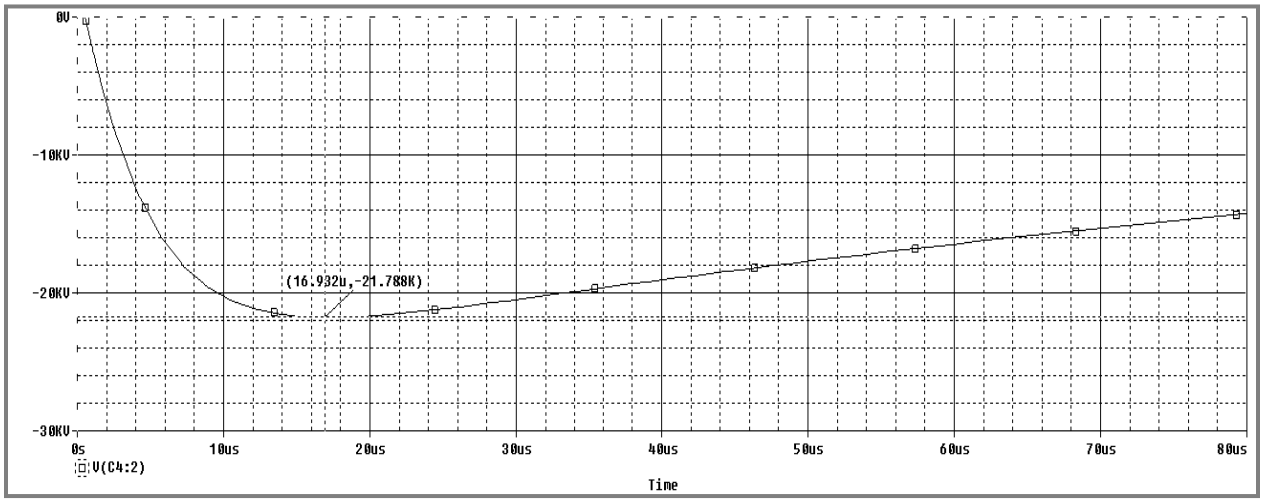

Figure4.51: Marx generator simulation with 1 unit of 0.22uF Capacitor (Without additional switch, both capacitor charging and discharging effect)

Figure 4.52: Marx generator simulation with 1 unit of 0.22uF Capacitor (With additional switch, capacitor charged and hold

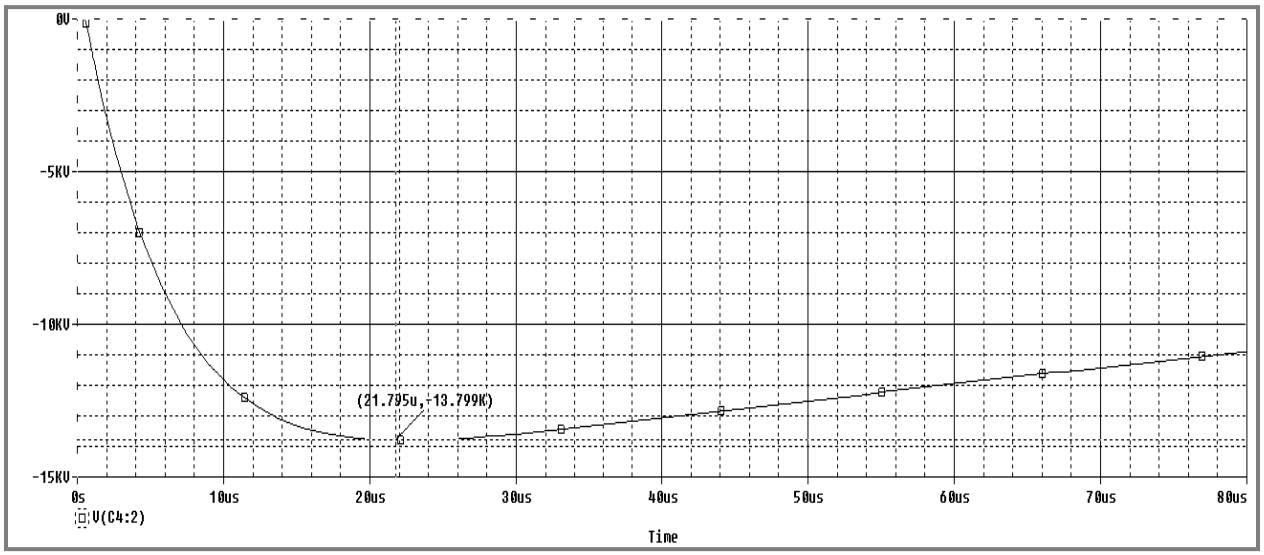

Figure4.53: Marx generator simulation with 2 units of 0.22uF Capacitor (Without additional switch, both capacitor charging and discharging effect)

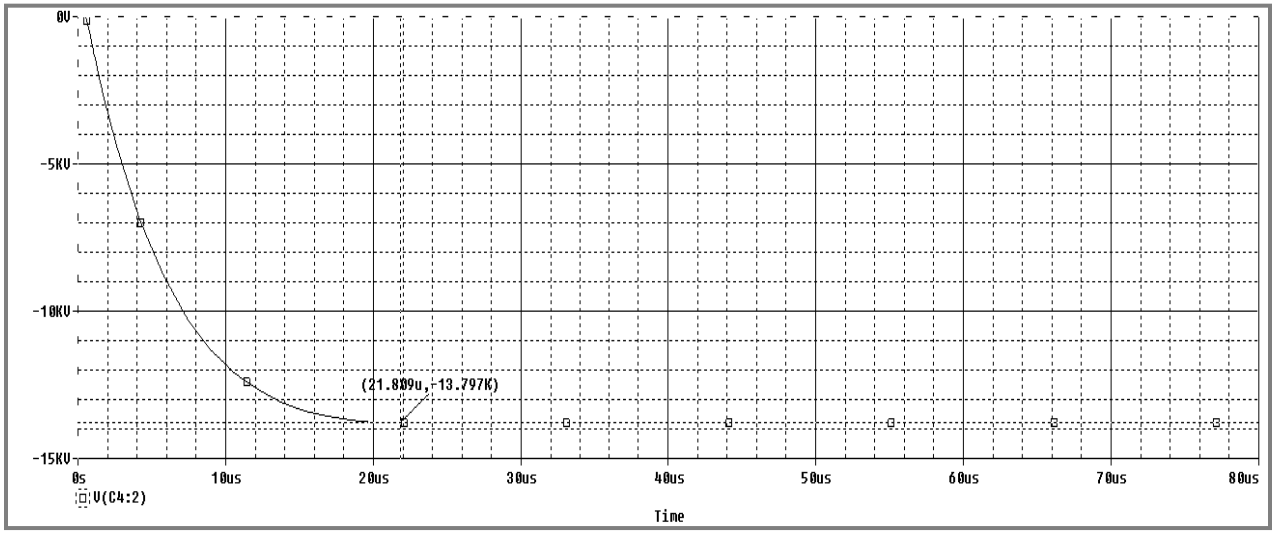

Figure4.54: Marx generator simulation with 2 unit of 0.22uF Capacitor (With additional switch, capacitor charged and hold)

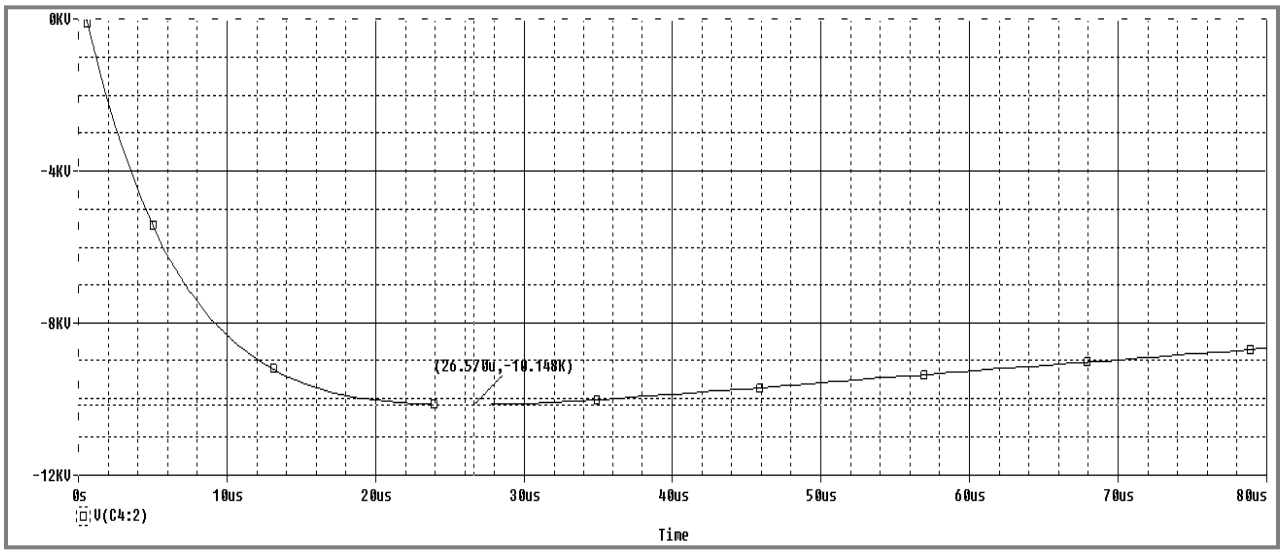

Figure4.55: Marx generator simulation with 3 units of 0.22uF Capacitor (Without additional switch, both capacitor charging and discharging effect)

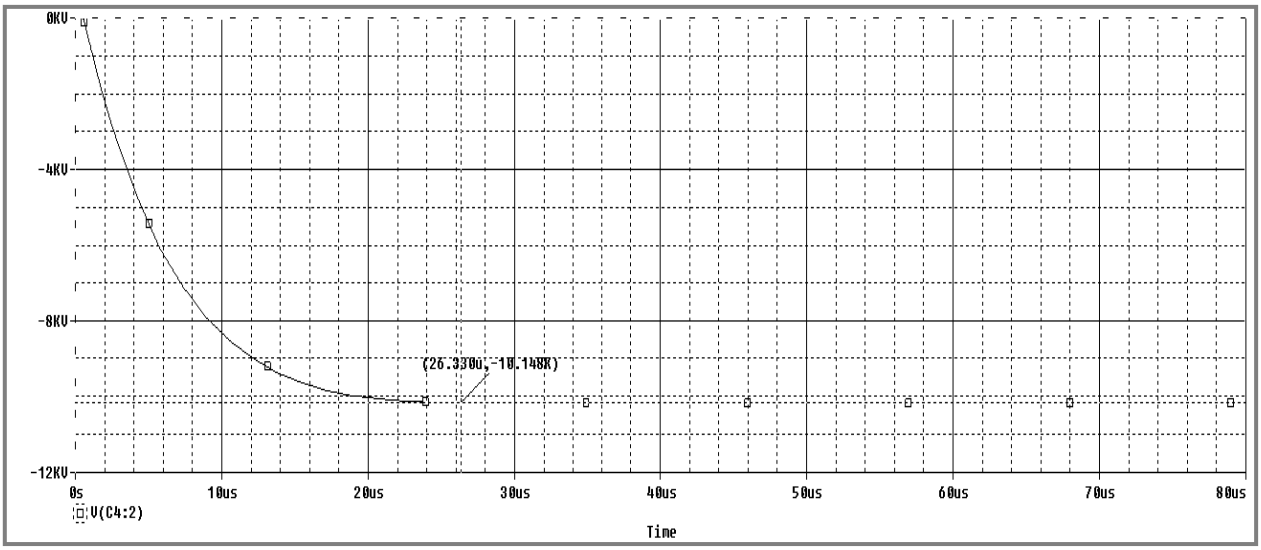

Figure4.56: Marx generator simulation with 3 unit of 0.22uF Capacitor (With additional switch, capacitor charged and hold)

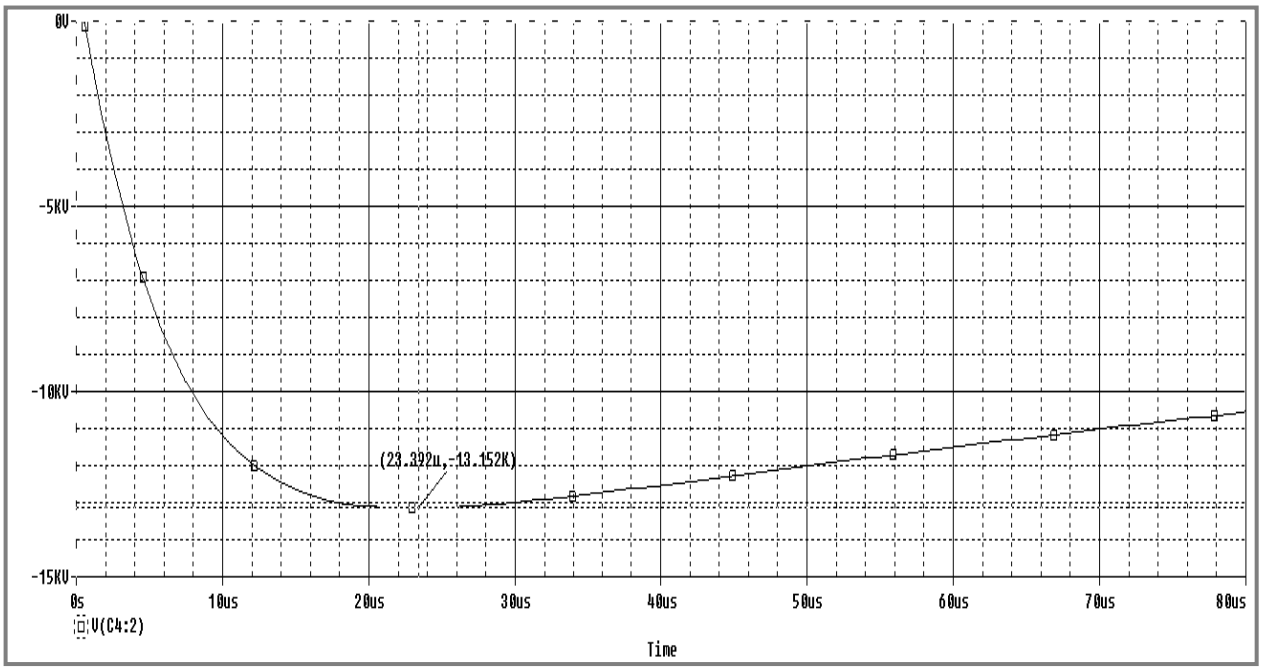

Figure4.57: Marx generator simulation with 1 units of 0.47uF Capacitor (Without additional switch, both capacitor charging and discharging effect)

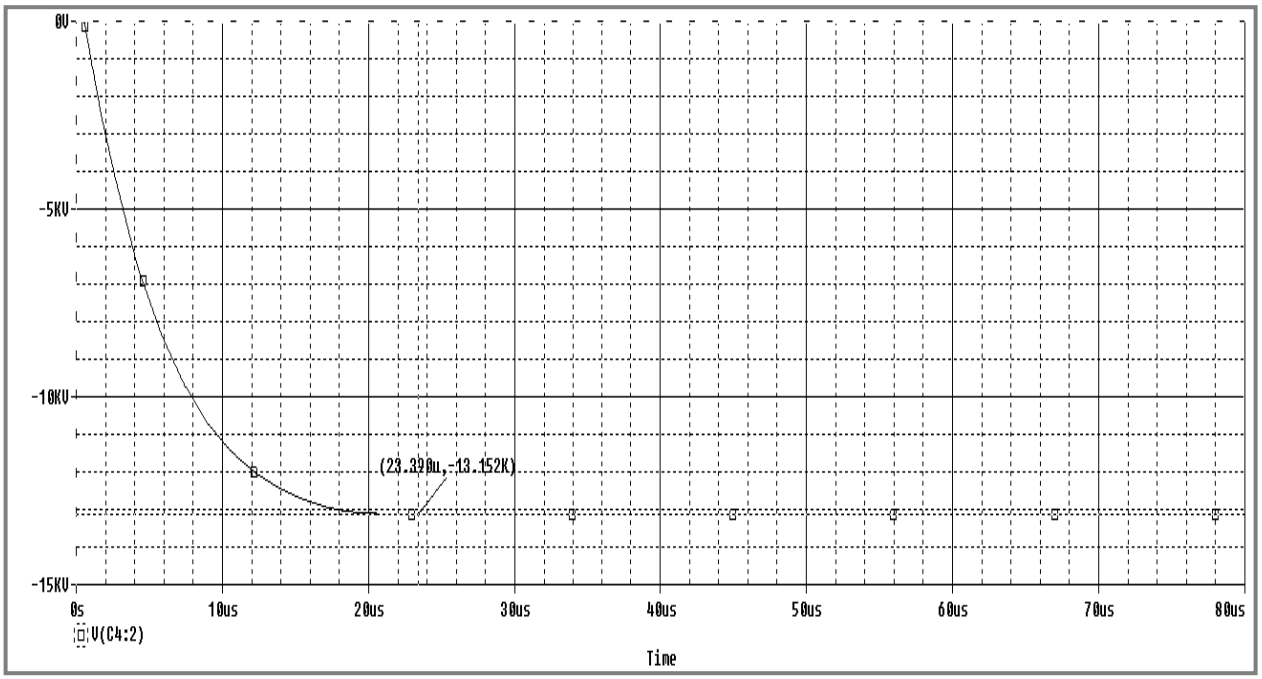

Figure4.58: Marx generator simulation with 1 unit of 0.47uF Capacitor (With additional switch, capacitor charged and hold)

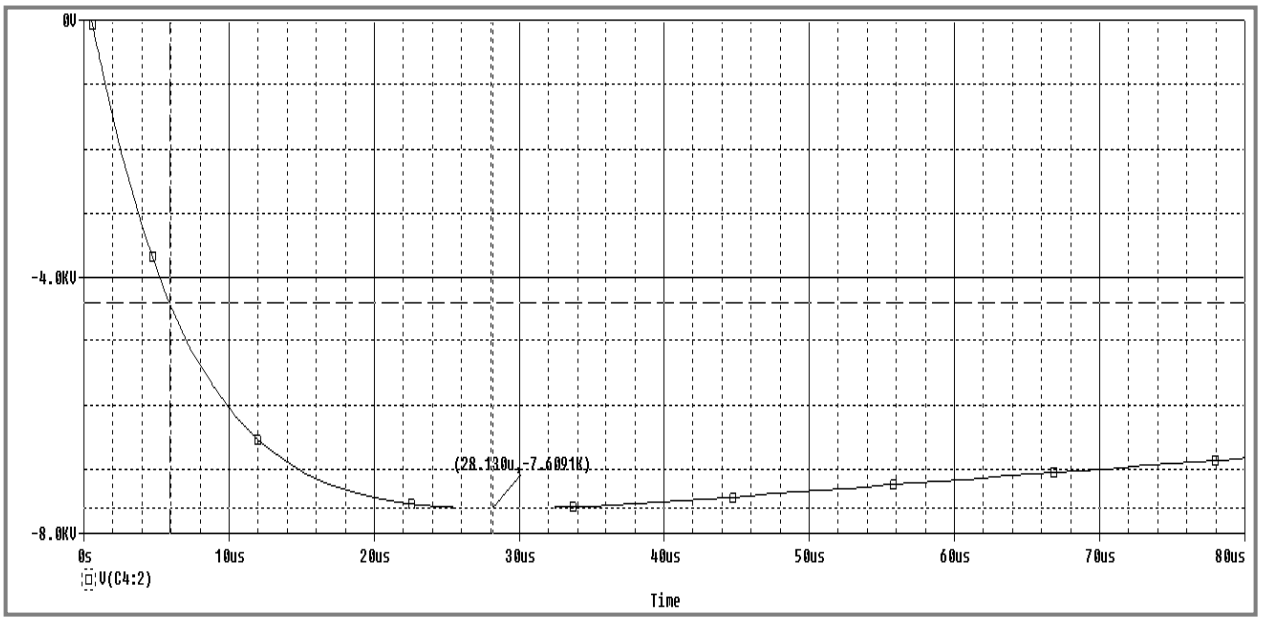

Figure4.59: Marx generator simulation with 2 units of 0.47uF Capacitor (Without additional switch, both capacitor charging and discharging effect)

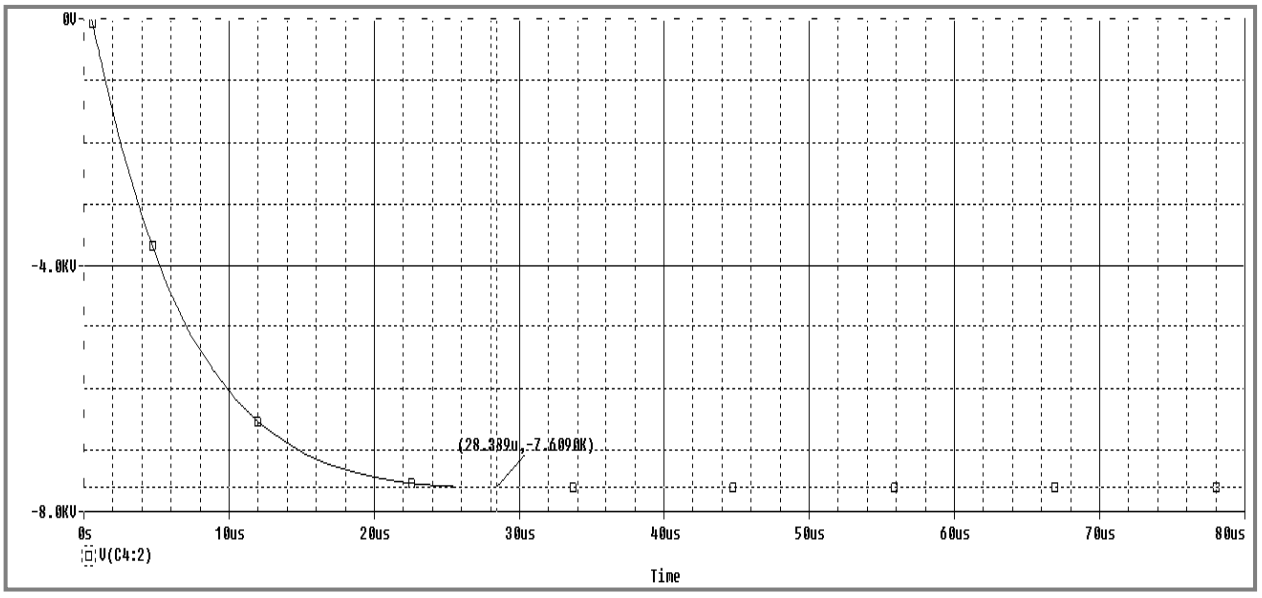

Figure4.60: Marx generator simulation with 2 units of 0.47uF Capacitor (With additional switch, capacitor charged and hold)

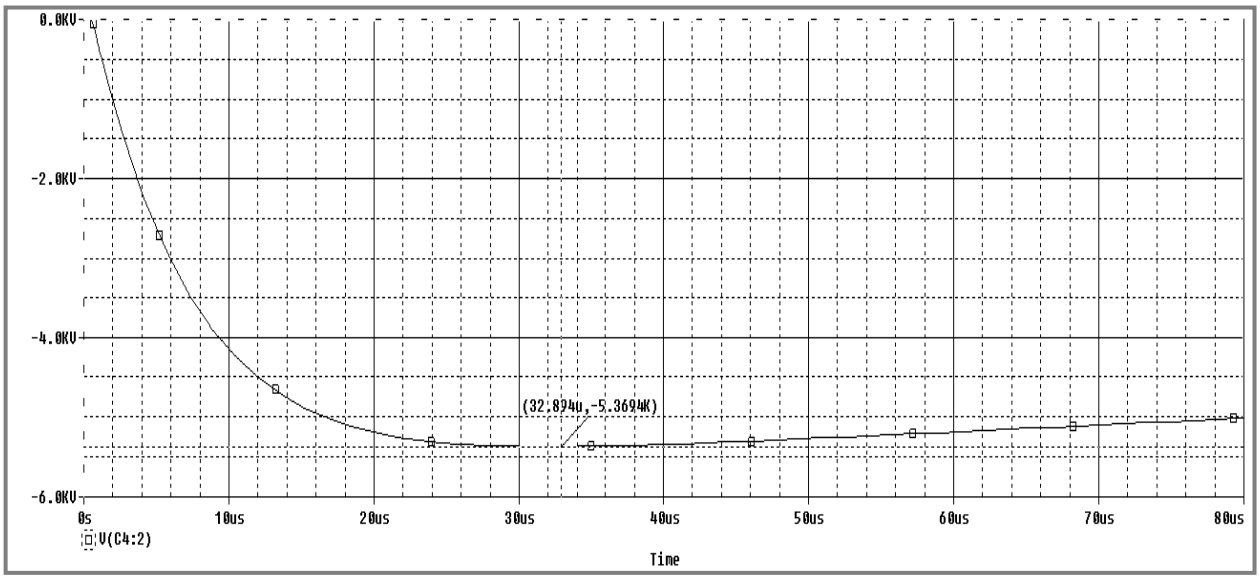

Figure4.61: Marx generator simulation with 3 units of 0.47uF Capacitor (Without additional switch, both capacitor charging and discharging effect)

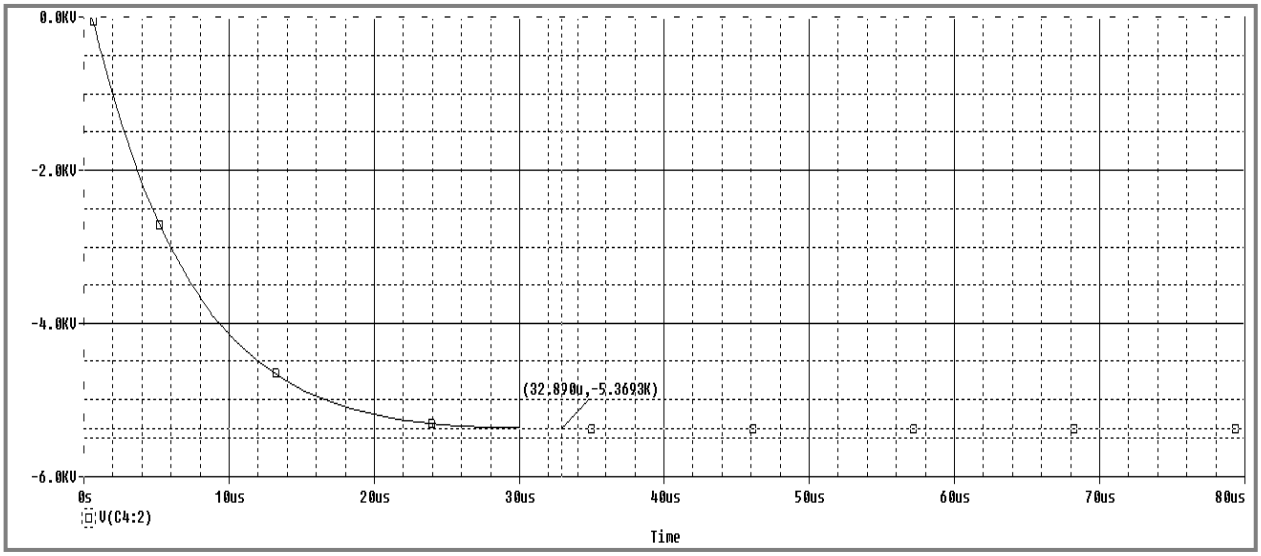

Figure4.62: Marx generator simulation with 3 units of 0.47uF Capacitor (With additional switch, capacitor charged and hold)

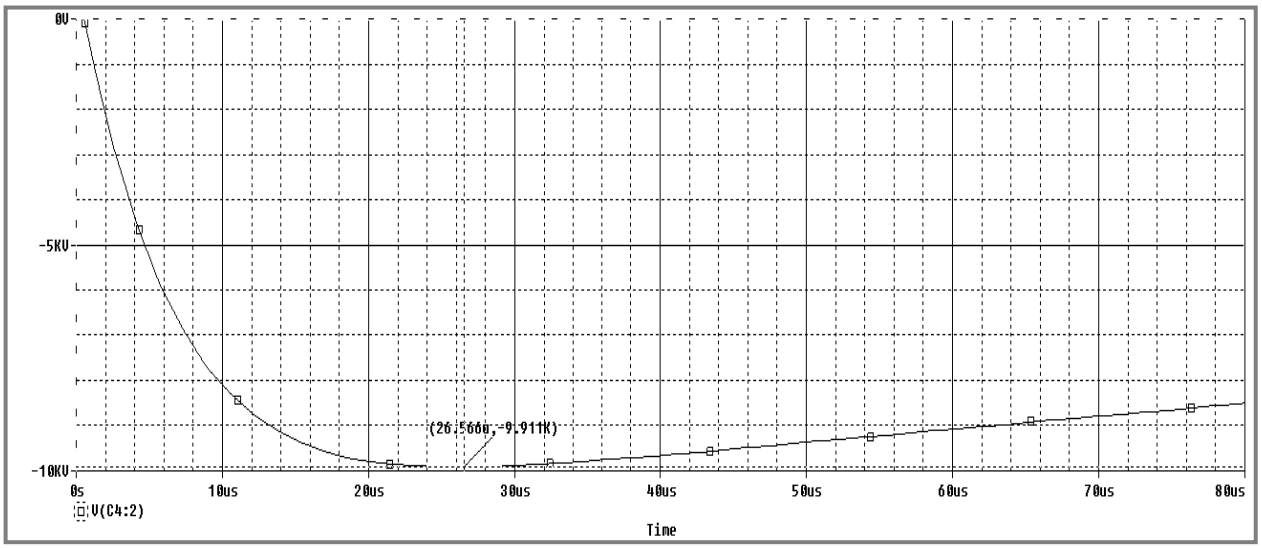

Figure4.63: Marx generator simulation with 1 units of 0.68uF Capacitor (Without additional switch, both capacitor charging and discharging effect)

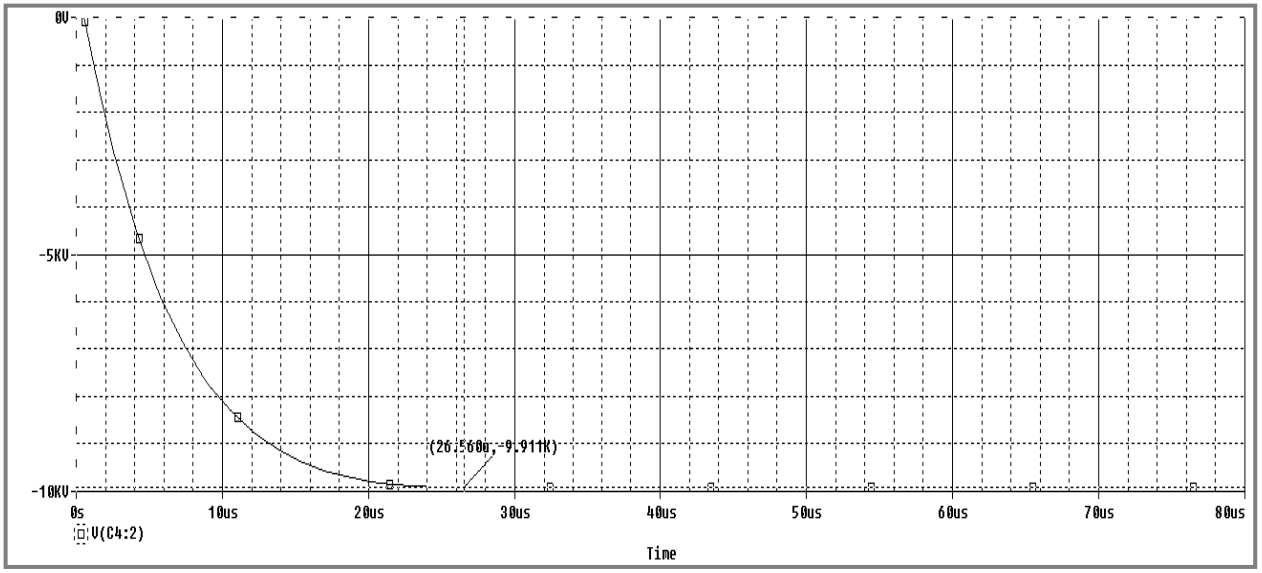

Figure4.64: Marx generator simulation with 1 units of 0.68uF Capacitor (With additional switch, capacitor charged and hold)

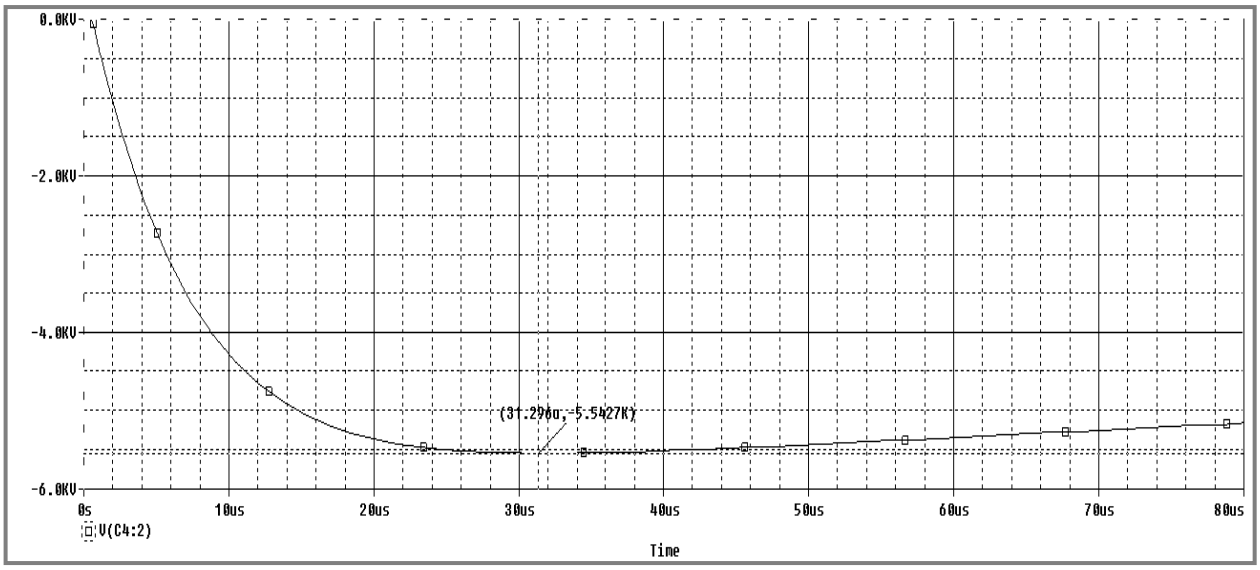

Figure4.65: Marx generator simulation with 2 units of 0.68uF Capacitor (Without additional switch, both capacitor charging and discharging effect)

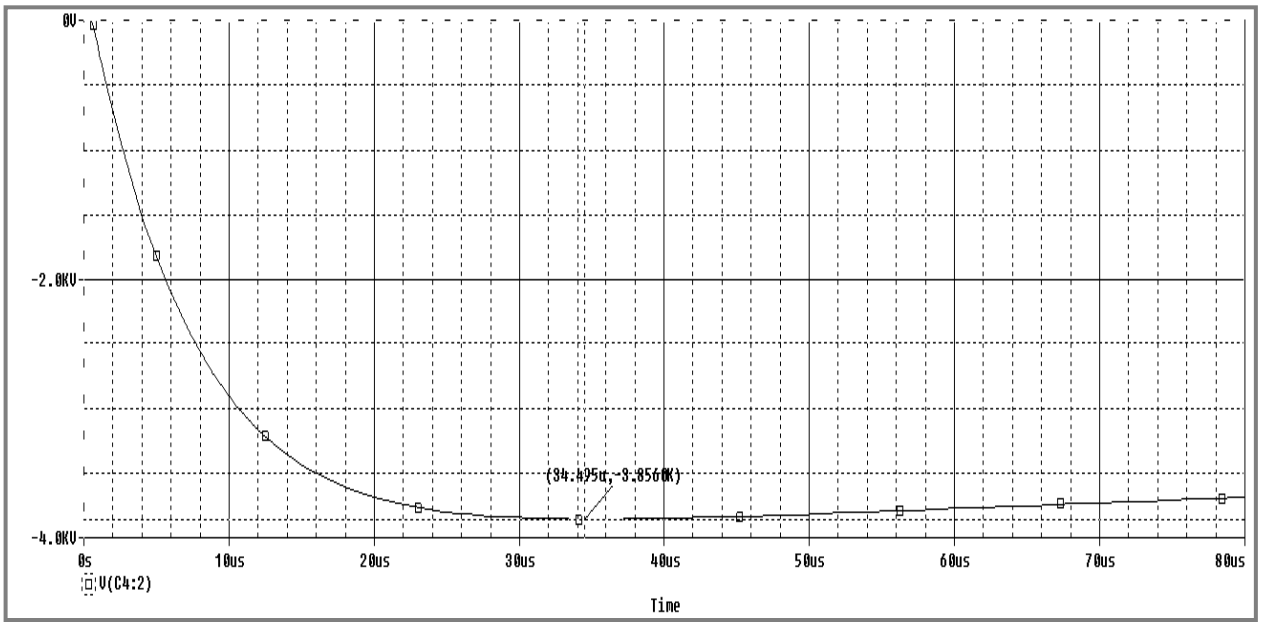

Figure4.66: Marx generator simulation with 2 units of 0.68uF Capacitor (With additional switch, capacitor charged and hold)

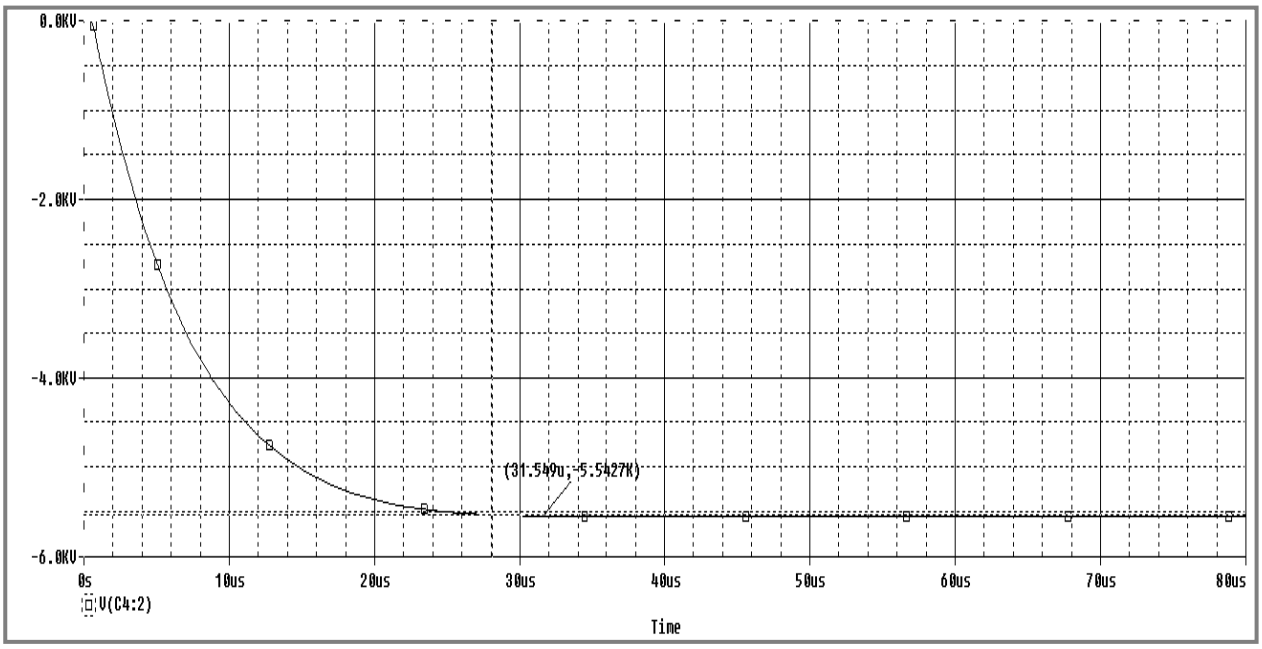

Figure4.67: Marx generator simulation with 3 units of 0.68uF Capacitor (Without additional switch, both capacitor charging and discharging effect)

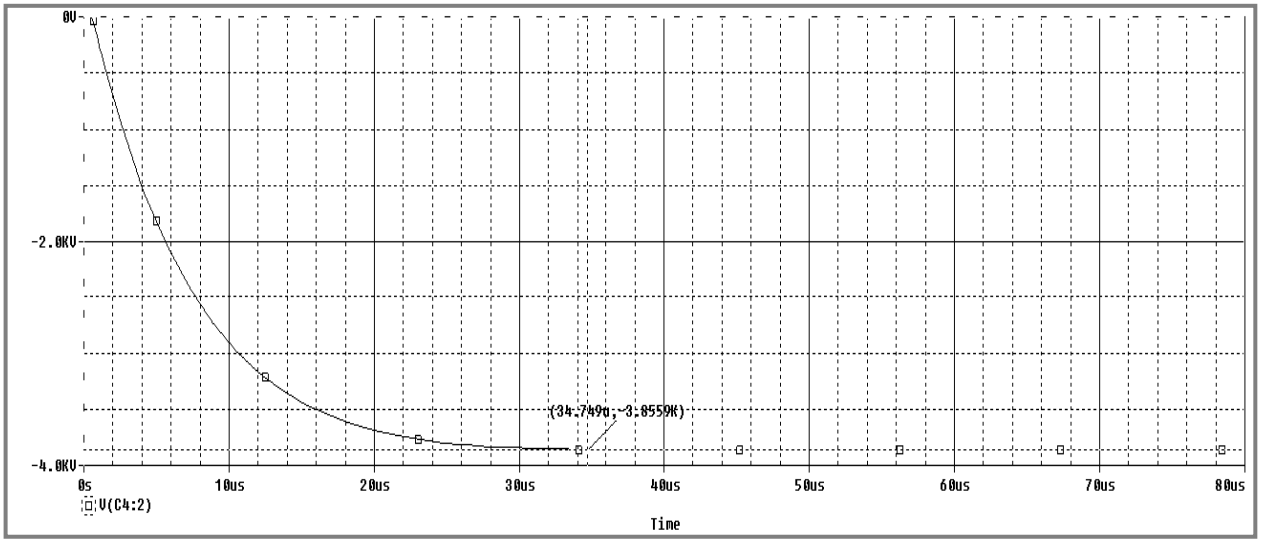

Figure4.68: Marx generator simulation with 2 units of 0.68uF Capacitor (With additional switch, capacitor charged and hold)

Results from the simulation is shown in the table

	1 unit of 0.22uF Capacitor	2 unit of 0.22uF Capacitor	3 unit of 0.22uF Capacitor
t_f (µs)	16.93	21.795	26.57
$\|V_{peak}\|$ (KV)	21.78	13.79	10.14

Table 1: Results found from the simulation with 0.22uF Capacitor

	1 unit of 0.47uF Capacitor	2 unit of 0.47uF Capacitor	3 unit of 0.47uF Capacitor
t_f (µs)	23.39	28.13	32.89
$\|V_{peak}\|$ (KV)	13.15	7.6	5.36

Table 2: Results found from the simulation with 0.47uF Capacitor

	1 unit of 0.68uF Capacitor	2 unit of 0.68uF Capacitor	3 unit of 0.68uF Capacitor
t_f (µs)	26.56	31.29	34.49
$\|V_{peak}\|$ (KV)	9.91	5.54	3.85

Table 3: Results found from the simulation with 0.68uF Capacitor

Analyzing the data, it is found that, if $C_{Storage}$increase, t_f(front time) increase

And for Peak Voltage, if $C_{Storage}$increase, V_{peak}decrease.

With the increment of $C_{Storage}$, Voltage drop across R_7 is too high. That is why, for high Capacitance value, Peak Voltage is very low.

CHAPTER 5

Conclusion

Objective of this study was to develop a small scale system for laboratory testing, as well as a simulation based proposition for the overall system for detection and store the energy from lightning. For this purpose, as a mock lightning source, marx generator is used. For the storage purpose, Metalized Polypropylene Film Capacitor is used. Simulation of mock lightning signal, through a switch to the storage capacitor is done in PSpice. IGBT is used for fast switching. High Speed Switching Circuit is developed to drive the IGBT and control the storage capacitor charging and discharging. High speed switching circuit contains microcontroller, gate drive, IGBT switch, storage capacitor. PWLIN function generator is used to produce the lightning signal in proteusisis simulation. For the detection part, Lab view program is used for simulation. Infrasonic detection system is used for the detection simulation.

References

[1]. Cummins K. L, Krider E.P & Malone M.D. The U.S. National Lightning Detection NetworkTM and Applications of Cloud-to-Ground Lightning Data by Electric Power Utilities, *"IEEE TRANSACTIONS ON ELECTROMAGNETIC COMPATIBLITY",VOL-40,*NOVEMBER 1998

[2]. Yang Z & Jiang S, Design of Lightning detection System Based on ARM, *International Conference on Lightning Protection (ICLP), Shanghai, China, 2014*

[3] Yanjie W, Changyuan F, Yiding L&Baoqiang W, Design of Lightning Location System Based on Photon and Infrasound Detection, *The Eighth International Conference on Electronic Measurement and Instruments ICEMI(*2007)

[4] Singh Y, Tripathi S &Pandey M, Analysis of Digital IIR Filter with LabVIEW, *International Journal of Computer Applications (0975 – 8887)Volume 10– No.6, November, (2010)*

[5] Basar M.F.M., Jamaluddin M.H, ZainudddinH.Jidin A., Aras M.Design and Development of A Small Scale System for Harvesting the Lightning Stroke Using the Impulse Voltage Generator at HV Lab, UTeM

[6] Nystrom S, Global Lightning Dataset Maps Lightning flashes anywhere in the World,Editor-in-Chief/Vaisala/Helsinki, Finland (2009)

[7] R.H. Golde. *Lightning,* Vols I and II. Academic Press, London/New York/San Francisco, 1977.

[8]Les Renardieres Group. Positive discharges in long air gaps at Les Renardieres.*Electra* No. 53, July 1977.

[9] *IEEE Standard Techniques for High-voltage Testing*,IEEEStd 4,1995

[10]M.E. Steven, "*An Impulse Generator Simulation Circuit,"* M.S Thesis Dept. EET, Miami Univ,Miami,1977

[11] Kuffel. E, Zaengl. W. S, "High Voltage Engineering Fundamentals", Newnes, Elsevier, Woburn, 1984.

[12] Suthar. J. L, Laghari. J. R, Saluzzo. T. J, "Usefulness of Spice in High Voltage Engineering Education", *Transactions on power system,* Vol.6 (August 1991): pp. 1272- 1278.

[13] Zhou. J. Y. and Boggs. S. A., "Low Energy Single Stage High Voltage Impulse Generator", *IEEE Transactions on Dielectrics and Electrical Insulation*, Vol.11 (August 2004): pp.507-603.

[14] Naidu and V. Kamaraju, "High Voltage Engineering," New Delhi: Tata McGraw-Hill, 1995.

[15] Gallagher. T. J, and Pearmain. A. J, "High Voltage Measurement, Testing and Design*", John Wiley & Sons Ltd,* 1983, p. 105

[16] M. Jolly, "Modeling and Simulation of Impulse Voltage Generator using Marx Circuit," M.S. thesis, Dept. Electrical Eng., National Institute of tech., Rourkela, Odisha, 2014

[17]Mohd, F. B.Lada M. Y. and Hasim N. (2011). Lightning Energy: A Lab Scale System,Energy Storage in the Emerging Era of Smart Grids, Prof. Rosario Carbone (Ed.), ISBN: 978-953-307-269-2,InTech, Available from: http://www.intechopen.com/books/energy-storage-in-the-emerging-era-of-smartgrids/lightning-energy-a-lab-scale-system

[18] Atmel Corporation, ATmega16 Datasheet, available from https://www.google.com/url?sa=t&rct=j&q=&esrc=s&source=web&cd=1&cad=rja&uact=8&ved=0ahUKEwjWp8yamZjMAhXHlZQKHYtVCosQFggjMAA&url=http%3A%2F%2Fwww.atmel.com%2Fimages%2Fdoc2466.pdf&usg=AFQjCNGtLH16aMl6wBBC6CNCBAcS1rxtQA

[19] International IOR Rectifier, IRG4PH50UD Datasheet, available from https://www.google.com/url?sa=t&rct=j&q=&esrc=s&source=web&cd=1&cad=rja&uact=8&ved=0ahUKEwiv3K_cmZjMAhUBxZQKHVeDDMIQFggcMAA&url=http%3A%2F%2Fwww.irf.com%2Fproduct-info%2Fdatasheets%2Fdata%2Firg4ph50ud.pdf&usg=AFQjCNGBNF6HIirInAzoaNl93egmB0BG5Q

[20] Uman, M.A. (1994). Natural Lightning. IEEE Transactions on Industry Applications, Vol.30,Issue.3, (June 1994), pp. 785-790, ISSN 0093-9994

[21] Farriz, M.B.,Herman, J.M., Jidin, A. &Zulkurnain, A.M.(2010)A New Source of Renewable Energy fromLightning Stroke: A Small Scale System, International Power Electronics Conference